

Entanglement Reactivation in Separable Environments

Stefano Pirandola

Computer Science, University of York, York YO10 5GH, United Kingdom

Combining two entanglement-breaking channels into a correlated-noise environment restores the distribution of entanglement. Surprisingly, this reactivation can be induced by the injection of separable correlations from the composite environment. In any dimension (finite or infinite), we can construct classically-correlated “twirling” environments which are entanglement-breaking in the transmission of single systems but entanglement-preserving when two systems are transmitted. Here entanglement is simply preserved by the existence of decoherence-free subspaces. Remarkably, even when such subspaces do not exist, a fraction of the input entanglement can still be distributed. This is found in separable Gaussian environments, where distillable entanglement is able to survive the two-mode transmission, despite being broken in any single-mode transmission by the strong thermal noise. In the Gaussian setting, entanglement restoration is a threshold process, occurring only after a critical amount of correlations has been injected. Such findings suggest new perspectives for distributing entanglement in realistic environments with extreme decoherence, identifying separable correlations and classical memory effects as physical resources for “breaking entanglement-breaking”.

PACS numbers: 03.65.Ud, 03.67.-a, 42.50.-p

I. INTRODUCTION

Entanglement is a fundamental physical resource in quantum information and computation [1, 2]. Once two remote parties, say Alice and Bob, share a suitable amount of entanglement, they can implement a variety of powerful protocols, including teleportation of quantum states [3, 4] and quantum gates [5], and the distribution of unconditionally secure keys [6, 7]. The problem of entanglement distribution is therefore a central topic of investigation in the quantum information community. Unfortunately, this distribution is also fragile: Quantum systems inevitably interact with the external environment whose decoherent action typically degrades their entanglement. In realistic implementations where the effect of decoherence is non-negligible, entanglement distribution may become challenging and may need distillation protocols [8, 9], where a large number of weakly-entangled states are converted into fewer but more entangled states.

The worst case scenario is when decoherence is so strong as to destroy any input entanglement. Mathematically, this is represented by the concept of entanglement-breaking channel [10, 11]. In general, a quantum channel \mathcal{E} is entanglement-breaking when its local action on one part of a bipartite state always results into a separable output state, no matter what the initial state were. In other words, given two systems, A and B , in an arbitrary bipartite state ρ_{AB} , the output state $\rho_{AB'} = (\mathcal{I}_A \otimes \mathcal{E}_B)(\rho_{AB})$ is always separable, where \mathcal{I}_A is the identity channel applied to system A and \mathcal{E}_B is the entanglement-breaking channel applied to system B .

Despite entanglement-breaking channels having been the subject of an intensive study by the community, they have only been analyzed under Markovian conditions of no memory. In other words, when the distribution involves two or more systems, these systems are typically assumed to be perturbed in an independent fashion, each of them subject to the same memoryless channel. For in-

stance, consider the symmetric scheme in Fig. 1, where a middle station (Charlie) has a bipartite system AB in some entangled state, but its communication lines with two remote parties (Alice and Bob) are affected by entanglement-breaking channels \mathcal{E}_A and \mathcal{E}_B .

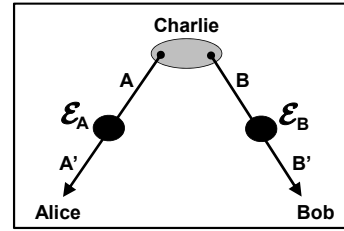


FIG. 1: Symmetric distribution in a memoryless environment. Charlie is the middle station with an entangled state of systems A and B . The communication lines with Alice and Bob are affected by two independent entanglement-breaking channels, \mathcal{E}_A and \mathcal{E}_B . In this environment, no entanglement can be distributed, neither via single transmission (Charlie \rightarrow Alice or Bob), nor via double (Charlie \rightarrow Alice and Bob).

Under the assumption of memoryless channels, there is clearly no way to distribute entanglement among any of the parties. Suppose that Charlie tries to share entanglement with one of the remote parties by sending one of the two systems while keeping the other (a scenario that we call “1-system transmission” or just “single transmission”). For instance, Charlie may keep system A while transmitting system B to Bob. The action of $\mathcal{I}_A \otimes \mathcal{E}_B$ destroys the initial entanglement, so that systems A (kept) and B' (transmitted) are separable. Symmetrically, the action of $\mathcal{E}_A \otimes \mathcal{I}_B$ destroys the entanglement between system A' (transmitted) and system B (kept). Now suppose that Charlie sends system A to Alice and system B to Bob (a scenario that we call “2-system transmission” or “double transmission”). Since the joint action of the two channels is given by the tensor product

$\mathcal{E}_A \otimes \mathcal{E}_B = (\mathcal{E}_A \otimes \mathcal{I}_B)(\mathcal{I}_A \otimes \mathcal{E}_B)$ quantum entanglement must necessarily be destroyed. In other words, since we have 1-system entanglement-breaking, then we must have 2-system entanglement-breaking.

In this paper we discuss how the previous implication is false when we introduce correlations, i.e., a memory, between the two entanglement-breaking channels. In the presence of a correlated-noise environment, the double transmission can successfully distribute entanglement despite the single transmission being subject to entanglement-breaking: Charlie can transmit entanglement to Alice and Bob, despite not being able to share any entanglement with them. Surprisingly, this effect can be induced by the presence of separable correlations in the joint environment, so that the broken entanglement is restored in a subtle way and it is not just replaced by other entanglement coming from the environment. In other words, to achieve this effect we do not need to consider arbitrary joint dilations of the two channels, but just two independent unitary dilations which are coupled by a separable environmental state.

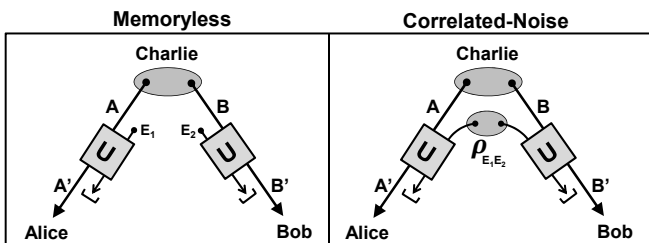


FIG. 2: *Left panel.* Symmetric distribution in a memoryless environment. The two entanglement-breaking channels, \mathcal{E}_A and \mathcal{E}_B , are dilated in two independent unitaries, $U_{E_1 A}$ and $U_{E_2 B}$, combining the input systems with two environmental systems, E_1 and E_2 , described by a product-state $\rho_{E_1} \otimes \rho_{E_2}$ (see text for more details). *Right panel.* Symmetric distribution in a correlated-noise environment. Here we create correlations between the two entanglement-breaking channels. The cheapest way is to replace $\rho_{E_1} \otimes \rho_{E_2}$ with a separable state $\rho_{E_1 E_2}$. In this scenario, despite entanglement cannot be distributed by single transmissions (Charlie cannot be entangled with Alice or Bob), still it can be distributed via the double transmission (so that Alice and Bob can become entangled). This reactivation of entanglement distribution is induced by the separable correlations injected from the environment. For twirling environments (in any dimension), the separable state $\rho_{E_1 E_2}$ is also classical (zero-discord), so that entanglement reactivation is mediated by purely-classical correlations.

To better clarify these points, consider Fig. 2. In the left panel, the two memoryless entanglement-breaking channels, \mathcal{E}_A and \mathcal{E}_B , are dilated in two unitaries, $U_{E_1 A}$ and $U_{E_2 B}$, coupling the input systems, A and B , with environmental systems, E_1 and E_2 , described by a product-state $\rho_{E_1} \otimes \rho_{E_2}$. In other words, the reduced state $\rho_A = \text{Tr}_B(\rho_{AB})$ is transformed by the map

$$\mathcal{E}_A(\rho_A) = \text{Tr}_{E_1}[U_{E_1 A}(\rho_{E_1} \otimes \rho_A)U_{E_1 A}^\dagger], \quad (1)$$

and, similarly, $\rho_B = \text{Tr}_A(\rho_{AB})$ is transformed as

$$\mathcal{E}_B(\rho_B) = \text{Tr}_{E_2}[U_{E_2 B}(\rho_{E_2} \otimes \rho_B)U_{E_2 B}^\dagger]. \quad (2)$$

Now, we note that there are many ways in which we can correlate the two channels. One could consider a completely general joint unitary U_{ABE} involving both the input systems, together with ancillary systems $\mathbf{E} = E_1 E_2 \dots$. However this general approach is not interesting and somehow trivial, since it always includes cases where the input entanglement is broken ($\rho_{A'B}$ and $\rho_{AB'}$ both separable) and replaced by fresh entanglement coming from the environment (so that $\rho_{A'B'}$ is entangled).

More interestingly, our analysis regards more realistic scenarios where the environment has minimal resources, i.e., it is weakly correlated, therefore far from being entangled. This is interesting for its potential applications to realistic non-Markovian systems, and theoretically non-trivial, since no swapping of entanglement can occur between systems and environment. In other words, we are interested in studying the weakest models of correlated-noise environment, close to the memoryless paradigm, which are able to reactivate the entanglement distribution.

Driven by such a goal, the simplest and cheapest way to combine two entanglement breaking channels and create a weakly-correlated joint environment, is to keep the previous independent unitaries, $U_{E_1 A}$ and $U_{E_2 B}$, and replace the environmental product-state $\rho_{E_1} \otimes \rho_{E_2}$ with a separable state $\rho_{E_1 E_2}$ having the same marginals $\rho_{E_1} = \text{Tr}_{E_2}(\rho_{E_1 E_2})$ and $\rho_{E_2} = \text{Tr}_{E_1}(\rho_{E_1 E_2})$, but correlated $\rho_{E_1 E_2} \neq \rho_{E_1} \otimes \rho_{E_2}$ (see the right panel of Fig. 2). Assuming this minimal dilation, we create a joint channel $\mathcal{E} = \mathcal{E}_{AB}$, transforming the input state ρ_{AB} as

$$\mathcal{E}(\rho_{AB}) = \text{Tr}_{E_1 E_2}[W(\rho_{E_1 E_2} \otimes \rho_{AB})W^\dagger], \quad (3)$$

where $W := U_{E_1 A} \otimes U_{E_2 B}$. Clearly, the joint channel is not memoryless $\mathcal{E} \neq \mathcal{E}_A \otimes \mathcal{E}_B$. Also note that the two local channels, \mathcal{E}_A and \mathcal{E}_B , are still well defined. For instance, if only system A is transmitted, we have

$$\begin{aligned} \rho_{A'B} &= (\mathcal{E}_A \otimes \mathcal{I}_B)(\rho_{AB}) \\ &= \text{Tr}_{E_1}[(U_{E_1 A} \otimes I_B)(\rho_{E_1} \otimes \rho_{AB})(U_{E_1 A}^\dagger \otimes I_B)]. \end{aligned} \quad (4)$$

In our work we show that, despite \mathcal{E}_A and \mathcal{E}_B being entanglement-breaking ($\rho_{A'B}$ and $\rho_{AB'}$ separable for any input ρ_{AB}), the joint channel \mathcal{E} is able to transmit entanglement, in the sense that $\rho_{A'B'}$ can be entangled for a suitable choice of the input entangled state ρ_{AB} . This entanglement reactivation is clearly an effect of the injected correlations, coming from the separable state of the environment $\rho_{E_1 E_2}$. As mentioned earlier, the interesting point is that the distribution is restored as an effect of weak, local-type correlations.

The reactivation of entanglement occurs in different kinds of separable environments, with rather different physical properties. The simplest environments to construct are the ‘‘twirling environments’’, which are based

on the twirling operators $U \otimes U$ (or $U \otimes U^*$). In this case, a random unitary U is directly applied to system A and the same unitary (or its conjugate) is correspondingly applied to system B . While the local action of a random unitary ($U \otimes I$ or $I \otimes U$) is entanglement-breaking, the correlated action ($U \otimes U$) perfectly preserves specific classes of entangled states, belonging to an invariant decoherence-free subspace of the joint correlated environment [15]. Since these environments are based on local operations and classical communication (LOCC), they are expected to introduce correlations which are separable and, more precisely, purely-classical. This feature can be explicitly checked by performing the unitary dilation of these environments according to Eq. (3), and checking that the environmental state $\rho_{E_1 E_2}$ is a classical state, therefore, with zero quantum discord.

Twirling environments can easily be constructed for quantum systems with Hilbert spaces of any dimension, both finite (qudits) and infinite (continuous-variable systems [13, 14]). In the case of two qudits, the randomization of the twirling operators $U \otimes U$ (or $U \otimes U^*$) is performed over the entire unitary group. In this case, it is easy to identify states which are invariant under $U \otimes U$ -twirling (Werner states [18]) and $U \otimes U^*$ -twirling (isotropic states [19]). In the specific case of qubits ($d = 2$), we can restrict the randomization to the basis of the Pauli operators, with the qubit Werner state being invariant under Pauli twirling.

Things are less trivial for infinite dimension, in particular, for bosonic modes [13, 14]. In this case, we restrict the twirling operators to the compact group of orthogonal symplectic transformations, i.e., phase-space rotations. The bosonic twirling environment so defined is non-Gaussian. Here, it is interesting to see that, only for the $U \otimes U^*$ -twirling, we can identify Gaussian states which are invariant and entangled: These are the two mode squeezed vacuum states, also known as Einstein-Podolsky-Rosen (EPR) states [14, 20]. More generally, this class can be extended to continuous variable Werner states, which are non-Gaussian states given by mixing an EPR state with a tensor product of thermal states [21].

Thanks to the existence of an invariant subspace of entangled states, twirling channels allow for the perfect distribution of entanglement in the two-system transmission, despite being one-system entanglement-breaking. However, the presence of such a subspace is not necessary if we relax the condition of perfect transmission and we accept that only a fraction of the input entanglement survives the two-system transmission. Remarkably, this is possible for bosonic systems evolving in a realistic model of correlated-noise Gaussian environment, which is the direct generalization of the standard thermal-lossy environment.

Our model of Gaussian environment can be represented by two beam-splitters ($U_{E_1 A}$ and $U_{E_2 B}$) whose environmental ports are subject to a correlated (separable) two-mode thermal state $\rho_{E_1 E_2}$. Such an environment does not have decoherence-free subspaces, apart from the

trivial invariant space given by its own thermal state $\rho_{E_1 E_2}$. Then, for a sufficiently large amount of entanglement at the input, Charlie can distribute a distillable amount to Alice and Bob, despite the single quantum channels Charlie-Alice (\mathcal{E}_A) and Charlie-Bob (\mathcal{E}_B) being entanglement-breaking. In particular, we find a threshold behavior according to which remote entanglement is restored only after a critical amount of correlations has been injected by the environment. Once this reactivation has taken place, we may ask if the amount of remote entanglement is then increasing in the amount of injected correlations. Unfortunately such a simple monotonicity does not seem to hold in the general case.

In fact, for these Gaussian environments, we adopt Gaussian discord as a measure of quantum correlations (upper bound to the actual discord). Then, we can easily evaluate the number of entanglement bits (ebits) which are remotely distributed in terms of the number of discordant bits (dbits) and classical bits (cbits), which are injected by the environment. For some classes of Gaussian environments, remote entanglement is proven to be increasing in the injected correlations (both classical and quantum). However, this monotonic behavior is not a general property, since we can exhibit two examples of environments, with identical classical correlations and increasing Gaussian discord, for which the number of ebits remotely restored is strictly decreasing. Because of this non-monotonic behavior, the phenomenon of entanglement restoration in Gaussian environments does not seem to be easily or directly related to a specific quantification of the correlations (classical, quantum or total).

To clarify relations with previous literature, we remark that our study is specifically devoted to show the potentialities of separable correlations in breaking the mechanism of entanglement-breaking, so that an entangled state is able to keep some of the initial entanglement during the transmission towards remote parties. It is clear that this is different from what considered in previous studies [70–73], where separable probes were used to distribute “fresh entanglement” between two quantum systems that have never interacted before. This basic difference leads to completely different roles for quantum discord. While in Refs. [70–73] discord is identified as the fundamental physical resource needed to distribute fresh entanglement, in our study discord is not necessary in general, since purely-classical correlations can indeed be sufficient to restore broken entanglement (e.g., see twirling environments).

In terms of potential impact, our work opens new possibilities for entanglement distribution in environments with extreme decoherence, where the presence of noise correlations and memory effects can be exploited to recover from entanglement-breaking. Since entanglement restoration can be achieved by separable correlations, our work also poses fundamental questions on the intimate relations between local and nonlocal correlations and, more generally, between classical and quantum correlations. It is important to note that memory channels and

correlated (in particular, non-Markovian) environments are present in a wide series of practical scenarios [22], including spin chains [23], atoms in optical cavities [24], quantum dots in photonic crystals [25], photonic propagation through linear optical systems [26–29] and atmospheric turbulence [30–32].

The general structure of the paper is the following. In Sec. II, we study twirling environments showing how entanglement is perfectly restored by classical correlations. This is proven for quantum systems of any dimension (qubits, qudits and bosonic systems). In Sec. III, we consider bosonic Gaussian environments. Here distillable entanglement can be restored by separable correlations, whose composition in terms of classical correlations and Gaussian discord is also analyzed. Finally, Sec. IV is for conclusion and discussion. For the sake of completeness, we also include an Appendix A, containing simple technical proofs, and an Appendix B, which is a brief review on bosonic systems and Gaussian states.

II. ENTANGLEMENT PRESERVATION IN TWIRLING ENVIRONMENTS

In this first analysis, we combine two entanglement-breaking channels to form a twirling environment, where entanglement distribution is reactivated by the presence of classical correlations. In particular, two-system transmission from Charlie to Alice and Bob allows for a perfect transfer of entanglement, thanks to the existence of an invariant subspace of entangled states. As already said, this is proven for Hilbert spaces of any dimension. In Sec. IIA, we start by considering the transmission of qubits in the simplest examples of twirling environments (correlated Pauli environments). Then, we consider the general case of qudits evolving in multidimensional twirling environments (Sec. IIB). Finally, we consider bosonic systems subject to non-Gaussian twirling environments which are based on random phase-space rotations (Sec. IIC).

A. Qubits in correlated Pauli environments

The simplest example can be constructed for qubits considering the basis of the four Pauli operators I , X , $Y = iXZ$ and Z [1]. Given an arbitrary two-qubit state ρ_{AB} , we consider the correlated Pauli channel

$$\mathcal{E}(\rho_{AB}) = \sum_{k=0}^3 p_k (P_k \otimes P_k) \rho_{AB} (P_k \otimes P_k)^\dagger, \quad (5)$$

where $P_k \in \{I, X, Y, Z\}$ and p_k are probabilities. This channel is clearly simulated by random LOCCs. In fact, it is equivalent to extract a random variable $K = \{k, p_k\}$, apply the Pauli unitary P_k to qubit A , communicate k and then apply the same unitary P_k to qubit B . It is easy to check that the two-qubit channel of Eq. (5) does not

change if we replace the Pauli twirling operator $P_k \otimes P_k$ with the alternative operator $P_k \otimes P_k^*$.

It is easy to write the unitary dilation of the correlated Pauli channel. It is sufficient to introduce an environment composed by two systems E_1 and E_2 , each being a qudit with dimension $d = 4$ and orthonormal basis $\{|k\rangle\}_{k=0}^3$. Then, we can write the dilation of Eq. (3), where the environment is prepared in the correlated state

$$\rho_{E_1 E_2} = \sum_{k=0}^3 p_k |k\rangle_{E_1} \langle k| \otimes |k\rangle_{E_2} \langle k|, \quad (6)$$

and the unitary interactions are control-Pauli unitaries,

$$U_{E_1 A} = \sum_{k=0}^3 |k\rangle_{E_1} \langle k| \otimes P_k, \quad U_{E_2 B} = \sum_{k=0}^3 |k\rangle_{E_2} \langle k| \otimes P_k. \quad (7)$$

As evident from Eq. (6), the state of the environment is separable, which means that only separable (i.e., local-type) correlations are injected into the travelling qubits. More precisely, since $\rho_{E_1 E_2}$ is expressed as a convex combination of orthogonal projectors, it is a purely-classical state, i.e., a state with zero quantum discord [34]. As a result, this environment contains correlations which are not only local but also purely classical.

We now show the conditions under which the correlated Pauli environment is simultaneously one-qubit entanglement-breaking and two-qubit entanglement-preserving. We start by considering the transmission of one qubit only, e.g., qubit A . This is subject to a depolarizing channel

$$(\mathcal{E}_A \otimes \mathcal{I}_B)(\rho_{AB}) = p_0 \rho_{AB} + \sum_{k=1}^3 p_k (P_k \otimes I) \rho_{AB} (P_k^\dagger \otimes I). \quad (8)$$

It is easy to show that \mathcal{E}_A is entanglement-breaking when $p_k \leq 1/2$ for every k (see Appendix A1 for a simple proof). A particular choice can be $p_0 \leq 1/2$ and $p_1 = p_2 = p_3 = (1 - p_0)/3$ as for instance used in Ref. [35].

Assuming the condition of one-qubit entanglement-breaking ($p_k \leq 1/2$), Charlie is clearly not able to share any entanglement with Alice or Bob. Despite this, Charlie can still distribute entanglement to Alice and Bob. This is possible because we can identify a class of entangled states ρ_{AB} which are invariant under the action of the correlated map (5), i.e., $\mathcal{E}(\rho_{AB}) = \rho_{AB}$. This class is simply given by the Werner states

$$\rho_{AB}(\gamma) := (1 - \gamma) \frac{I_{AB}}{4} + \gamma |-\rangle_{AB} \langle -|, \quad (9)$$

with parameter $-1/3 \leq \gamma \leq 1$, where $I_{AB}/4$ is the maximally-mixed state and

$$|-\rangle_{AB} = \frac{1}{\sqrt{2}} (|0\rangle_A |1\rangle_B - |1\rangle_A |0\rangle_B) \quad (10)$$

is the maximally-entangled (singlet) state. For $\gamma > 1/3$, the state $\rho_{AB}(\gamma)$ is known to be entangled and distillable.

The remarkable property of the Werner states is that they are invariant under twirling operators $U \otimes U$, i.e.,

$$(U \otimes U)\rho_{AB}(\gamma)(U \otimes U)^\dagger = \rho_{AB}(\gamma), \quad (11)$$

for any unitary U . As a result, they are clearly invariant under the action of the correlated Pauli environment of Eq. (5). Thus, if Charlie sends Werner states with $\gamma > 1/3$, these entangled states are perfectly distributed to Alice and Bob (two-qubit entanglement-preserving).

B. Qudits in multidimensional twirling environments

In this section, we consider the general case of qudits, i.e., quantum systems with Hilbert space of arbitrary dimension $d \geq 2$. For these systems, we can easily construct classically-correlated environments which are simultaneously 1-qudit entanglement-breaking and 2-qudit entanglement-preserving.

Consider two qudits, A and B , with Hilbert spaces of the same dimension d and prepared in a bipartite state ρ_{AB} . A multidimensional $U \otimes U$ twirling channel is described by the following completely-positive trace-preserving map

$$\mathcal{E}_{UU}(\rho_{AB}) = \int_{\mathcal{U}(d)} dU (U \otimes U)\rho_{AB}(U \otimes U)^\dagger, \quad (12)$$

where the integral is over the entire unitary group $\mathcal{U}(d)$ acting on the d -dimensional Hilbert space, and dU is the Haar measure. This channel is clearly realizable by random LOCCs: A random unitary U is drawn and applied to qudit A , the choice of U is classically communicated to the other qudit B , which is then subject to the same unitary. Similarly, we can define a $U \otimes U^*$ twirling channel, by replacing the twirling operator $U \otimes U$ with the alternative twirling $U \otimes U^*$ in the definition of Eq. (12). Compactly, we refer to the $U \otimes V$ twirling channel

$$\mathcal{E}_{UV}(\rho_{AB}) = \int_{\mathcal{U}(d)} dU (U \otimes V)\rho_{AB}(U \otimes V)^\dagger, \quad (13)$$

where $V = U$ or $V = U^*$.

This channel can be dilated to introduce an environmental system. Since we have an integral in Eq. (13), this dilation seems to involve the introduction of continuous variable systems. In fact, the unitary group $\mathcal{U}(d)$ is labelled by d^2 real parameters [36], which means that $2d^2$ continuous variable systems are needed to embed these parameters and describe the environment. Actually, such a continuous dilation is not necessary, since we can always replace the previous Haar integral with a discrete sum over a finite number of suitably-chosen unitaries. In fact, any twirling channel (13) can be written as

$$\mathcal{E}_{UV}(\rho_{AB}) = \frac{1}{K} \sum_{k=0}^{K-1} (U_k \otimes V_k)\rho_{AB}(U_k \otimes V_k)^\dagger, \quad (14)$$

where U_k belongs to the set of unitary 2-design \mathcal{D} [37, 38] and $V_k = U_k$ or $V_k = U_k^*$. The set \mathcal{D} has a finite number of elements which depends of the dimension of the Hilbert space $K = K(d)$ (to see how the cardinality K scales with the dimension d , see Ref. [39]). The proof of the equivalence between Eqs. (13) and (14) can be found in Ref. [37] for the $U \otimes U$ twirling channel. See Appendix A 2 for a simple extension of the proof to the other $U \otimes U^*$ twirling channel. Note that, in the case of qubits ($d = 2$), an example of unitary 2-design is provided by the Clifford group [37, 40], which is the normalizer of the Pauli group and typically employed in quantum error correction [41, 42].

Now using the unitary 2-design, we can dilate the twirling channel into an environment made by finite-dimensional systems, i.e., two larger qudits E_1 and E_2 , each with dimension K and orthonormal basis $\{|k\rangle\}_{k=0}^{K-1}$. In other words, for $\mathcal{E}_{UV}(\rho_{AB})$ we can write the dilation of Eq. (3), where the environment is prepared in the uniformly-correlated state

$$\rho_{E_1 E_2} = \frac{1}{K} \sum_{k=0}^{K-1} |k\rangle_{E_1} \langle k| \otimes |k\rangle_{E_2} \langle k|, \quad (15)$$

and the interactions are the following control-unitaries

$$U_{E_1 A} = \sum_{k=0}^{K-1} |k\rangle_{E_1} \langle k| \otimes U_k, \quad U_{E_2 B} = \sum_{k=0}^{K-1} |k\rangle_{E_2} \langle k| \otimes V_k, \quad (16)$$

where $U_k \in \mathcal{D}$ and $V_k = U_k$ or $V_k = U_k^*$. As evident from Eq. (15), the state of the environment is separable and purely-classical (zero discord). As expected, twirling environments only contain purely-classical correlations.

Once we have fully characterized the properties of these environments, we show the conditions under which they are simultaneously one-qudit entanglement-breaking and two-qudit entanglement-preserving. First of all, we explicitly show that one-qudit transmission is always subject to entanglement-breaking. In fact, suppose that Charlie transmits qudit A to Alice while keeping qudit B . For any input state ρ_{AB} , the output state is given by

$$(\mathcal{E}_A \otimes \mathcal{I}_B)(\rho_{AB}) = \int_{\mathcal{U}(d)} dU (U \otimes I)\rho_{AB}(U^\dagger \otimes I) = \frac{I}{d} \otimes \text{Tr}_A(\rho_{AB}). \quad (17)$$

It is clear that the random map $U \otimes I$ implements an entanglement-breaking channel (a symmetric result holds for the other random map $I \otimes V$ which describes the transmission of qudit B). As shown in Appendix A 3, the proof of Eq. (17) is an application of the identity

$$\langle O \rangle_U := \int_{\mathcal{U}(d)} dU U O U^\dagger = \frac{\text{Tr}(O)}{d} I, \quad (18)$$

which is the Haar average of a linear operator O . In turn, Eq. (18) is a consequence of Schur's lemma and the invariance of the Haar measure [43].

The next step is the analysis of the two-qudit transmission, from Charlie to Alice and Bob. In this case, we look for entangled states which are preserved by the correlated action of the twirling environment. Luckily, we can easily find states which are invariant under the action of the twirling operator $U \otimes V$, i.e.,

$$(U \otimes V)\rho_{AB}(U \otimes V)^\dagger = \rho_{AB} . \quad (19)$$

Thanks to this invariance, such states are fixed points of the $U \otimes V$ twirling channel of Eq. (13).

In the specific case of $V = U$, it is well known that the unique solution of Eq. (19) is provided by the multidimensional Werner states [18]. For two qudits A and B (with the same dimension d), the Werner states are defined by the one-parameter class [18, 44]

$$\rho_{AB}(\mu) := \frac{1}{d^2 + d\mu}(I_{AB} + \mu V) \quad (20)$$

where $-1 \leq \mu \leq 1$, and V is the unitary flip operator $V|\varphi\rangle_A \otimes |\psi\rangle_B = |\psi\rangle_A \otimes |\varphi\rangle_B$. These states are known to be entangled and distillable for any physical value of $\mu < -d^{-1}$. Thus, if Charlie has a Werner state $\rho_{AB}(\mu)$ with suitable μ (in the entanglement regime), he is able to perfectly transmit this state to Alice and Bob, who can therefore share and distill entanglement. Such a distribution is possible, despite Charlie not being able to share any entanglement with Alice or Bob due to the entanglement-breaking condition of Eq. (17).

Coming back to Eq. (19), one can find a similar solution for $V = U^*$. In fact, as shown in Ref. [19], there exist states which are invariant under $U \otimes U^*$ -twirling. These are called isotropic states, and they are defined by the one-parameter class [19]

$$\rho_{AB}(\gamma) := (1 - \gamma)\frac{I_{AB}}{d^2} + \gamma|\psi\rangle_{AB}\langle\psi| , \quad (21)$$

involving a convex combination of the maximally mixed state $d^{-2}I_{AB}$ and the maximally entangled state

$$|\psi\rangle_{AB} = \frac{1}{\sqrt{d}} \sum_{k=0}^{d-1} |k\rangle_A |k\rangle_B , \quad (22)$$

with parameter $-(d^2 - 1)^{-1} \leq \gamma \leq 1$. In general, these states are entangled and distillable for any physical value of $\gamma > (1 + d)^{-1}$. Thus, if Charlie has an isotropic state $\rho_{AB}(\gamma)$ with suitable γ (i.e., in the entanglement regime), he is able to perfectly transmit this state to Alice and Bob, who therefore can share and distill entanglement. Again, this is possible despite the transmission of a single qudit being subject to an entanglement-breaking channel according to Eq. (17).

It is clear that these results can be specialized to the case of qubits ($d = 2$). For qubits, the classes of multidimensional Werner states of Eq. (20) and isotropic states of Eq. (21) coincide up to a local unitary [19]. Multidimensional Werner states reduce exactly to the qubit

Werner state of Eq. (9) which is $U \otimes U$ -invariant [80]. On the other hand, isotropic states reduce to Eq. (9), proviso that the singlet $|-\rangle_{AB}$ is replaced by the triplet

$$|+\rangle_{AB} = \frac{1}{\sqrt{2}}(|0\rangle_A |0\rangle_B + |1\rangle_A |1\rangle_B) . \quad (23)$$

This state is now $U \otimes U^*$ -invariant and known as Werner-like state (this definition is commonly adopted when the singlet is replaced by another maximally entangled state). If we restrict the random unitaries to the basis of the Pauli operators $\{P_k\}$ as done in Sec. II A, we see that both these states are fixed points of the correlated Pauli environment of Eq. (5), since this map does not change under the replacement $P_k \otimes P_k \rightarrow P_k \otimes P_k^*$.

C. Bosonic systems in non-Gaussian twirling environments

Here we extend the analysis to the case of continuous variable systems, i.e., quantum systems with infinite dimensional Hilbert spaces ($d = \infty$). In particular, we consider the case of two bosonic modes of the electromagnetic field (see Appendix B for a brief review of the main concepts on bosonic systems). The simplest generalization of the notion of twirling environment involves the use of rotations in the phase space. Given a single bosonic mode with number operator \hat{n} , the rotation operator is defined as $R_\theta = \exp(-i\theta\hat{n})$. In the phase space, the symplectic action of this operator is described by the rotation matrix

$$\mathbf{R}_\theta = \begin{pmatrix} \cos \theta & \sin \theta \\ -\sin \theta & \cos \theta \end{pmatrix} . \quad (24)$$

In terms of the second-order statistical moments, we have that the covariance matrix (CM) \mathbf{V} of the input mode is transformed by the congruence

$$\mathbf{V} \rightarrow \mathbf{R}_\theta \mathbf{V} \mathbf{R}_\theta^T . \quad (25)$$

Now, given an input state ρ_{AB} of two modes, A and B , we can synchronize two random rotations and define the bosonic twirling channel as

$$\mathcal{E}_{\theta\theta'}(\rho_{AB}) = \int \frac{d\theta}{2\pi} (R_\theta \otimes R_{\theta'})\rho_{AB}(R_\theta \otimes R_{\theta'})^\dagger , \quad (26)$$

where $R_{\theta'} = R_\theta$ or $R_{\theta'} = R_{-\theta} = R_\theta^*$. This is a non-Gaussian channel, since the twirling operator $R_\theta \otimes R_{\theta'}$, despite Gaussian, is averaged using a uniform (i.e., non-Gaussian) distribution. It is clearly based on random LOCCs, since random rotations are locally applied to each bosonic mode and can be correlated by means of classical communication.

It is interesting that the unitary dilation of this channel can be restricted to a finite-dimensional environment.

This is because the single-mode rotation operator R_θ belongs to the compact subgroup of the orthogonal symplectic transformations $\mathcal{K}(2) = \mathcal{Sp}(2) \cap \mathcal{O}(2)$ (these correspond to passive Gaussian unitaries, i.e., unitary transformations preserving both the Gaussian statistics and the energy of the state). Then, $\mathcal{K}(2)$ is isomorphic to the unitary group $\mathcal{U}(1)$, which is the multiplicative group composed by all complex numbers with unit module, also known as the ‘‘circle group’’.

Because of this isomorphism, a unitary 2-design $\mathcal{D} \subset \mathcal{U}(1)$ can be mapped into a unitary 2-design for $\mathcal{K}(2)$ [39]. As a result, we can write

$$\mathcal{E}_{\theta\theta'}(\rho_{AB}) = \frac{1}{K} \sum_{k=0}^{K-1} (R_{\theta_k} \otimes R_{\theta'_k}) \rho_{AB} (R_{\theta_k} \otimes R_{\theta'_k})^\dagger, \quad (27)$$

for a suitable set of angles $\{\theta_0, \dots, \theta_{K-1}\}$, and $\theta'_k = \theta_k$ or $\theta'_k = -\theta_k$. In this form, the channel is manifestly non-Gaussian. In particular, it can be represented by introducing two environmental qudits, E_1 and E_2 , prepared in a correlated state $\rho_{E_1 E_2}$ as in Eq. (15), and interacting with the two bosonic modes by two control-unitaries as in Eq. (16), where now the target unitaries, U_k and V_k , are rotations in the phase space. The environmental state is not only separable but also purely-classical (zero discord), which means that only classical correlations are injected by the bosonic twirling environment.

It is easy to show that one-mode transmission is always subject to entanglement-breaking in this kind of environment. For instance, if mode A is transmitted from Charlie to Alice, then the output state

$$\rho_{A'B} = \int \frac{d\theta}{2\pi} (R_\theta \otimes I) \rho_{AB} (R_\theta \otimes I)^\dagger \quad (28)$$

is separable, no matter what the input state ρ_{AB} is. In fact, it is easy to prove that a uniformly dephasing channel as in Eq. (28) is entanglement-breaking. For completeness, we give this simple proof in Appendix A 4.

The next step is to find two-mode states which are invariant under bosonic twirling

$$(R_\theta \otimes R_{\theta'}) \rho_{AB} (R_\theta \otimes R_{\theta'})^\dagger = \rho_{AB}, \quad (29)$$

so that they are perfectly transmitted by the bosonic twirling environment

$$\mathcal{E}_{\theta\theta'}(\rho_{AB}) = \rho_{AB}. \quad (30)$$

Let us start this search within the set of zero-mean Gaussian states, therefore completely characterized by their CMs \mathbf{V}_{AB} . Finding a solution of Eq. (29) is therefore equivalent to solving

$$(\mathbf{R}_\theta \oplus \mathbf{R}_{\theta'}) \mathbf{V}_{AB} (\mathbf{R}_\theta \oplus \mathbf{R}_{\theta'})^T = \mathbf{V}_{AB}. \quad (31)$$

Depending on the type of environment, i.e., $\theta' = \theta$ (correlated rotations) or $\theta' = -\theta$ (anti-correlated rotations), we have two different classes of invariant Gaussian states.

Unfortunately, in the case of correlated rotations, the invariant Gaussian states are separable. In fact, it is easy to check that, for $\theta' = \theta$ and arbitrary θ , the unique solution of Eq. (31) is given by the quasi-normal form

$$\mathbf{V}_{AB} := \begin{pmatrix} \mathbf{A} & \mathbf{C} \\ \mathbf{C}^T & \mathbf{B} \end{pmatrix} = \begin{pmatrix} \alpha & \omega & \varphi \\ \omega & \alpha & -\varphi & \omega \\ \varphi & \omega & \beta & \omega \\ & & & \beta \end{pmatrix}, \quad (32)$$

with $\alpha, \beta \geq 1$ and ω, δ are real numbers (which must satisfy a set of bona-fide conditions in order to make the previous matrix a quantum CM [45]). Then, it is easy to check that the previous CM can describe separable Gaussian states only. See Appendix A 5 to see how to derive Eq. (32) and check its separability properties.

Thus, despite there are two-mode Gaussian states ρ_{AB} which are invariant under correlated rotations ($\theta' = \theta$), these states must be separable. This negative result can be generalized: No entangled Gaussian state is invariant under twirlings of the form $U \otimes U$, with U Gaussian unitary (apart from the trivial case $U = \pm I$). For a simple proof see Appendix A 6.

Luckily, the scenario is completely different when we consider the other type of environment. We can easily find entangled Gaussian states which are invariant under anti-correlated rotations. In fact, we can easily check that, for $\theta' = -\theta$ and arbitrary θ , a possible solution of Eq. (31) is given by the CM

$$\mathbf{V}_{AB}(\mu) := \begin{pmatrix} \mu \mathbf{I} & \mu' \mathbf{Z} \\ \mu' \mathbf{Z} & \mu \mathbf{I} \end{pmatrix}, \quad (33)$$

where

$$\mu \geq 1, \quad \mu' := \sqrt{\mu^2 - 1}, \quad (34)$$

and

$$\mathbf{I} = \begin{pmatrix} 1 & \\ & 1 \end{pmatrix}, \quad \mathbf{Z} = \begin{pmatrix} 1 & \\ & -1 \end{pmatrix}. \quad (35)$$

This is the CM of a two-mode squeezed vacuum state $\rho_{AB}(\mu)$, also known as EPR state [14]. Thus, in the presence of the anti-correlated environment $\mathcal{E}_{\theta(-\theta)}$, despite Charlie cannot share any entanglement with Alice or Bob (one-mode entanglement-breaking), he is still able to distribute them entanglement by transmitting EPR states perfectly (two-mode entanglement-preserving).

More generally, we can extend the previous analysis and include non-Gaussian input states in Charlie’s hands. One possible choice is the continuous-variable version of the Werner state [74]

$$\rho_{AB}(p, \mu) = p \rho_{AB}(\mu) + (1-p) [\rho_A(\mu) \otimes \rho_B(\mu)] \quad (36)$$

which corresponds to a mix, with probability p , of an EPR state $\rho_{AB}(\mu)$ and a tensor-product of two identical single-mode thermal states, $\rho_A(\mu)$ and $\rho_B(\mu)$, with

CMS $\mathbf{V}_A(\mu) = \mathbf{V}_B(\mu) = \mu\mathbf{I}$. This state is known to be entangled for [74]

$$p > p(\bar{n}) := \frac{1}{1 + 2 \coth(2 \operatorname{arcsinh} \sqrt{\bar{n}})}, \quad (37)$$

where $\bar{n} = (\mu - 1)/2$ is the mean number of thermal photons in each mode [for large \bar{n} , we have $p(\bar{n}) \rightarrow 1/3$, which reminds the threshold valid for qubit Werner states].

Since thermal states are invariant under phase-space rotations, the convex combination of Eq. (36) is invariant under the action of anti-correlated rotations $\theta' = -\theta$, therefore representing a fixed point of $\mathcal{E}_{\theta(-\theta)}$. As a result, any continuous-variable Werner state $\rho_{AB}(p, \mu)$ with $p > p(\bar{n})$ can be used to perfectly transmit entanglement to Alice and Bob, despite the environment $\mathcal{E}_{\theta(-\theta)}$ being one-mode entanglement-breaking.

III. ENTANGLEMENT RESTORATION IN CORRELATED-NOISE GAUSSIAN ENVIRONMENTS

In the previous Sec. II, we have studied the distribution of entanglement in twirling channels, considering quantum systems with Hilbert spaces of any dimension, both finite and infinite. We have shown the conditions under which these environments are simultaneously one-system entanglement-breaking and two-system entanglement-preserving. This peculiar situation is possible due to the existence of invariant subspaces of entangled states (Werner states and isotropic states). In this case, entanglement preservation is induced by the injection of purely-classical correlations in the travelling systems.

In this section, we consider a rather different scenario. We construct a correlated-noise Gaussian environment which generalizes the standard model of memoryless thermal-lossy environment to include cross-correlations between two travelling modes. This is done by using two beam-splitters which mix the travelling modes, A and B , with two environmental modes, E_1 and E_2 , prepared in a correlated Gaussian state $\rho_{E_1 E_2}$ (in particular, it can be chosen to be separable). Each single beam-splitter introduces losses and thermal noise such to realize an entanglement-breaking channel. For this reason, Charlie is not able to share any entanglement with Alice or Bob. Despite this, the noise-correlations enable Charlie to distribute entanglement to Alice and Bob. As we will show, an input EPR state ρ_{AB} with sufficiently-high EPR correlations is able to generate an output state which is entangled and even distillable by Alice and Bob.

This is remarkable considering that: (i) For these environments, there is no decoherence-free subspace of entangled states (which means that entanglement cannot be preserved); and (ii) Entanglement distribution can be reactivated by the injection of separable correlations (so that lost entanglement is not replaced by other entanglement, i.e., coming from the environment).

In detail, this section is structured as follows. In Sec. III A, we characterize our basic model of correlated-noise Gaussian environment, identifying the physical conditions under which it is separable or entangled (Sec. III A 1), and discussing specific kinds of quadrature correlations, that we call symmetric or asymmetric (Sec. III A 2). In Sec. III B, we study the distribution of entanglement. Assuming the condition of one-mode entanglement-breaking, we show how entanglement distribution can be restored by the environmental correlations (in particular, separable correlations) identifying the regime where remote entanglement is also distillable. We show that entanglement restoration is a threshold process starting only after a critical amount of correlations is present in the environment.

In particular, in Secs. III B 1 and III B 2, we specify this study to environments with symmetric and asymmetric correlations, analyzing the process of entanglement restoration in terms of the injected classical and quantum correlations. Here we compute the critical number of correlation bits (cbits and dbits) which are needed for entanglement restoration. Once reactivated, the number of ebits remotely restored is increasing in the number of correlation bits which are injected. This monotonic behavior holds true when we compare environments with the same types of correlations (symmetric or asymmetric) but fails to be true in the general case as explicitly discussed in Sec. III B 3.

Finally, in Sec. III B 4, we also analyze the evolution of the EPR correlations in this peculiar process. General notions and technical details on bosonic systems and Gaussian states can be found in Appendix B.

A. Characterization of Gaussian environments with correlated noise

In this section, we introduce and fully characterize our model of correlated-noise Gaussian environment, which represents the simplest and most direct generalization of the standard memoryless Gaussian environment with losses and thermal noise.

We consider a Gaussian decoherence process which affects two bosonic modes, A and B , in a symmetric way. In order to describe the introduction of losses and thermal noise, we consider two beam splitters (with the same transmissivity τ) which combine modes A and B with two environmental modes, E_1 and E_2 , respectively. These ancillary modes are prepared in a zero-mean Gaussian state $\rho_{E_1 E_2}$ which is symmetric under E_1 - E_2 permutation. In the standard memoryless model depicted in the left panel of Fig. 3, the environment is in a tensor-product state $\rho_{E_1 E_2} = \rho_{E_1} \otimes \rho_{E_2}$, meaning that E_1 and E_2 are fully independent. In particular, $\rho_{E_1} = \rho_{E_2}$ is a thermal state with covariance matrix (CM) $\omega\mathbf{I}$, where the noise variance $\omega = 2\bar{n} + 1$ quantifies the mean number of thermal photons \bar{n} entering the beam splitter. Each interaction is then equivalent to a lossy channel with transmissivity

τ and thermal noise ω .

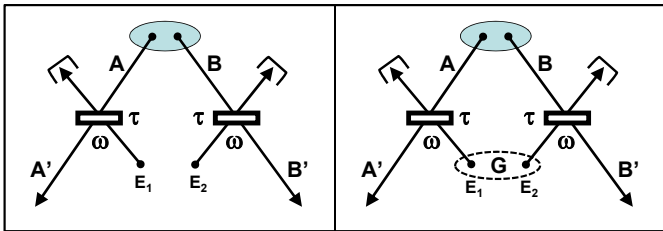


FIG. 3: Gaussian environments. *Left.* Memoryless Gaussian environment with losses τ and thermal noise ω . *Right.* Correlated-noise Gaussian environment, with losses τ , thermal noise ω and cross-correlations \mathbf{G} . The state of the environment $\rho_{E_1 E_2}$ can be separable or entangled.

In our work, we generalize this Gaussian process to include the presence of correlations between the environmental modes, as depicted in the right panel of Fig. 3. The simplest extension of the model consists of taking the ancillary modes, E_1 and E_2 , in a zero-mean Gaussian state $\rho_{E_1 E_2}$ with CM in the symmetric normal form

$$\mathbf{V}_{E_1 E_2}(\omega, g, g') = \begin{pmatrix} \omega \mathbf{I} & \mathbf{G} \\ \mathbf{G} & \omega \mathbf{I} \end{pmatrix}, \quad (38)$$

where $\omega \geq 1$ is the thermal noise variance associated with each ancilla, and the off-diagonal block

$$\mathbf{G} = \begin{pmatrix} g & \\ & g' \end{pmatrix} \quad (39)$$

accounts for the correlations between the ancillas. Such a correlated thermal state can be separable or entangled (explicit conditions will be given below), and its quantum discord is always non-zero (apart when $g' = g = 0$).

It is clear that, when we consider the two interactions $A-E_1$ and $B-E_2$ separately, the environmental correlations are washed away. In fact, by tracing out E_2 , we are left with mode E_1 in a thermal state ($\mathbf{V}_{E_1} = \omega \mathbf{I}$) which is combined with mode A via the beam-splitter. In other words, we have again a lossy channel with transmissivity τ and thermal noise ω . The scenario is identical for the other mode B when we trace out E_1 . However, when we consider the joint action of the two environmental modes, the correlation block \mathbf{G} comes into play and the global dynamics of the two travelling modes becomes completely different from the standard memoryless scenario.

Before studying the system dynamics and the corresponding evolution of entanglement, we need to characterize the correlation block \mathbf{G} more precisely. In fact, the two correlation parameters, g and g' , cannot be completely arbitrary but must satisfy specific physical constraints. These parameters must vary within ranges which make the CM of Eq. (38) a bona-fide quantum CM [45]. Given an arbitrary value of the thermal noise

$\omega \geq 1$, the correlation parameters must satisfy the following three bona-fide conditions

$$|g| < \omega, \quad |g'| < \omega, \quad \omega^2 + gg' - 1 \geq \omega |g + g'|. \quad (40)$$

(Details of the proof can be found in Appendix B3).

1. Separability properties

Once the bona-fide conditions for the environment are fully clarified, the next step is the characterization of its separability properties.

For this aim, we compute the smallest partially-transposed symplectic (PTS) eigenvalue ε_{env} associated with the CM of the environment $\mathbf{V}_{E_1 E_2}$ (for more details on this formalism see Appendix B3). For Gaussian states, this eigenvalue represents an entanglement monotone, being fully equivalent to the log-negativity [53]. After simple algebra, we get

$$\varepsilon_{\text{env}} = \sqrt{\omega^2 - gg' - \omega |g - g'|}. \quad (41)$$

Provided that the conditions of Eq. (40) are satisfied, the separability condition $\varepsilon_{\text{env}} \geq 1$ is equivalent to

$$\omega^2 - gg' - 1 \geq \omega |g - g'|. \quad (42)$$

The various conditions of bona-fide and separability can be combined together. An environment of the form (38) with thermal noise $\omega \geq 1$ is bona-fide and separable when the correlation parameters g and g' satisfy

$$|g| < \omega, \quad |g'| < \omega, \quad \omega^2 - 1 \geq \max\{\Gamma_-, \Gamma_+\}. \quad (43)$$

where

$$\Gamma_- := \omega |g + g'| - gg', \quad (44)$$

$$\Gamma_+ := \omega |g - g'| + gg'. \quad (45)$$

By contrast, it is bona-fide and entangled when

$$|g| < \omega, \quad |g'| < \omega, \quad \Gamma_- \leq \omega^2 - 1 < \Gamma_+. \quad (46)$$

To better clarify the structure of the environment, we provide a numerical example in Fig. 4. In the left panel of this figure, we consider the *correlation plan* which is spanned by the two parameters g and g' . For a given value of the thermal noise ω , we identify the subset of points which satisfy the bona-fide conditions of Eq. (40). This subset corresponds to the white area in the figure. Within this area, we then characterize the regions which correspond to separable environments (area labelled by S) and entangled environments (areas labelled by E).

2. Symmetric and asymmetric noise correlations

Here we specify our model of Gaussian environment to particular cases with specific correlation properties.

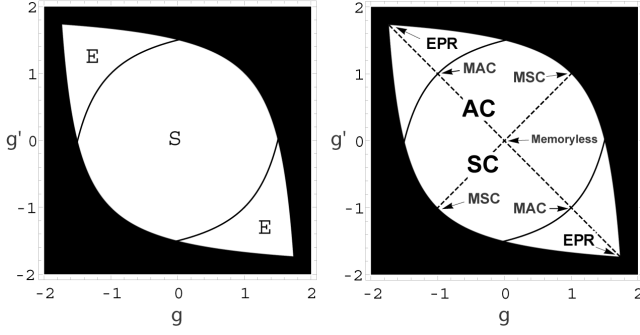


FIG. 4: *Left.* Correlation plan (g, g') for the Gaussian environment, corresponding to thermal noise $\omega = 2$. The black area identifies forbidden environments (correlations are too strong to be compatible with quantum mechanics). White area identifies physical environments, i.e., the subset of points which satisfy the bona-fide conditions of Eq. (40). Within this area, the inner region labelled by “S” identifies separable environments [Eq. (43) is satisfied] while the two outer regions labelled by “E” identify entangled environments [Eq. (46) is satisfied]. *Right.* Correlation plan where we display the memoryless environment (origin $g' = g = 0$), SC environments (bisector $g' = g$) and AC environments (bisector $g' = -g$). The MSC environments are the SC environments with maximal correlations (extremal points on the bisector $g' = g$). The EPR environments are the AC environments with maximal correlations (extremal points on the bisector $g' = -g$). Finally, the MAC environments are those AC environments which are simultaneously separable and maximally correlated.

Before discussing these cases, note that the memoryless Gaussian environment corresponds to the origin of the correlation plan ($g' = g = 0$), as also depicted in the right panel of Fig. 4. In particular, the memoryless environment represents the unique physical solution for $\omega = 1$ (vacuum noise), in correspondence to which all the correlation plan collapses into its origin. In the remainder of this section we implicitly take $\omega > 1$, therefore excluding the trivial case of a singular correlation plan.

The first type of specifically-correlated environment is called “symmetrically correlated” (SC). This corresponds to taking $g' = g$, which means that positions and momenta of the two modes, E_1 and E_2 , are correlated exactly in the same way. On the correlation plan, these environments are points on the bisectors of the first and third quadrants (see the right panel of Fig. 4).

It is easy to check that the bona-fide conditions of Eq. (40) simplify to the single inequality

$$|g| \leq \omega - 1, \quad (47)$$

with maximal symmetrical correlations (MSC) achieved at $g = \omega - 1$ and $g = 1 - \omega$, which are the two extremal points shown in the figure. It is important to note that SC environments are always separable, since Eq. (42) becomes $|g| \leq \sqrt{\omega^2 - 1}$, which is always satisfied by Eq. (47). Then, they are also mixed, with von Neumann entropy equal to

$$S_{SC}(\omega, g) = h(\omega + g) + h(\omega - g), \quad (48)$$

where [81]

$$h(x) := \frac{x+1}{2} \log\left(\frac{x+1}{2}\right) - \frac{x-1}{2} \log\left(\frac{x-1}{2}\right). \quad (49)$$

Given an arbitrary SC environment, we can investigate the nature of its separable correlations in terms of classical correlations (measured in classical bits or “cbits”) and Gaussian discord (measured in discordant bits or “dbits”). Using the formulas of Ref. [63] (see also Appendix B 5) we compute the amount of classical correlations which is here equal to

$$C = h(\omega) - h\left(\omega - \frac{g^2}{\omega + 1}\right), \quad (50)$$

and the amount of Gaussian discord D which is given by

$$D_{SC}(\omega, g) = h(\omega) + h\left(\omega - \frac{g^2}{\omega + 1}\right) - S_{SC}(\omega, g). \quad (51)$$

The bits of total correlations are quantified by the quantum mutual information $I = C + D$, here equal to

$$I_{SC}(\omega, g) = 2h(\omega) - S_{SC}(\omega, g). \quad (52)$$

It is important to note that Gaussian discord D is an upper bound to the actual discord, even if they are conjectured to coincide [65, 66]. Correspondingly, the measure for classical correlations which is here considered $C = I - D$ represents a lower bound to the actual amount of classical correlations.

As expected, both types of correlations, C and D , are increasing in $|g|$ at any fixed value of thermal noise ω . Despite increasing, Gaussian discord must be bounded by $D \leq 1$, which is compatible with the fact that SC environments are always separable ($D > 1$ is a sufficient condition for entanglement [63]). Finally, one can check [75] that MSC environments have maximal Gaussian discord not only between the SC environments but, more generally, among all the separable Gaussian environments, represented by the “S” region in Fig. 4.

The second type of environment, that we call “asymmetrically correlated” (AC), corresponds to the condition $g' = -g$. This means that positions and momenta have opposite correlations, i.e., if positions are correlated (anticorrelated), then momenta are anticorrelated (correlated). On the correlation plan, these environments are represented by the points lying on the bisectors of the second and fourth quadrants (see right panel of Fig. 4).

In this case, the bona-fide conditions of Eq. (40) simplify to the inequality

$$|g| \leq \sqrt{\omega^2 - 1}. \quad (53)$$

For maximal correlations $|g| = \sqrt{\omega^2 - 1}$ we have an EPR state, which is pure and maximally entangled. Depending on the sign of g , we have two different EPR environments: The positive EPR environment ($g = \sqrt{\omega^2 - 1}$)

with positions correlated, and the negative EPR environment ($g = -\sqrt{\omega^2 - 1}$) with positions anticorrelated. Apart from these extremal cases, AC environments are mixed with entropy

$$S_{AC}(\omega, g) = 2h\left(\sqrt{\omega^2 - g^2}\right). \quad (54)$$

In general, we note that AC environments can be separable or entangled. By using Eq. (42), we see that they are separable for

$$|g| \leq \omega - 1, \quad (55)$$

while they are entangled for stronger correlations

$$\omega - 1 < |g| \leq \sqrt{\omega^2 - 1}. \quad (56)$$

We call maximally-separable AC environments (MACs) those AC environments with maximal correlations but still separable. They are characterized by the border condition $|g| = \omega - 1$, and they correspond to the two intersection points shown in the right panel of Fig. 4.

As before, we can easily quantify the amounts of classical correlations C and Gaussian discord D , both increasing functions in $|g|$. For AC environments, these quantities are respectively given by Eq. (50) and

$$D_{AC}(\omega, g) = h(\omega) + h\left(\omega - \frac{g^2}{\omega + 1}\right) - S_{AC}(\omega, g). \quad (57)$$

The quantum mutual information is now equal to

$$I_{AC}(\omega, g) = 2h(\omega) - S_{AC}(\omega, g).$$

The correlation properties of the AC environments can be easily compared with those of the previous SC environments. For fixed values of ω and g with $|g| \leq \omega - 1$ (separable environments), AC and SC environments have identical classical correlations but different Gaussian discord, i.e.,

$$\delta D := D_{SC}(\omega, g) - D_{AC}(\omega, g) > 0. \quad (58)$$

This means that they also have different amounts of total correlations

$$\delta I := I_{SC}(\omega, g) - I_{AC}(\omega, g) > 0. \quad (59)$$

As clear from the previous formulas, this is simply a consequence of the fact that AC environments are more entropic than SC environments, i.e.,

$$\delta S := S_{SC}(\omega, g) - S_{AC}(\omega, g) < 0. \quad (60)$$

The difference in entropy directly quantifies the difference in the correlations between these environments

$$\delta D = \delta I = -\delta S. \quad (61)$$

However, contrary to the SC environments, the AC environments can also become entangled. When the correlation parameter g is chosen in the entanglement regime

of Eq. (56), classical correlations and Gaussian discord become larger (in particular, D may exceed 1). The optimum is reached at the two EPR states whose classical and quantum correlations are identical and maximal in the entire correlation plan. In particular, we have $C_{EPR} = D_{EPR} = h(\omega)$ which is just the entropy of entanglement of the EPR state.

B. Distribution and distillation of entanglement in correlated-noise Gaussian environments

Let us study the propagation of entanglement in a correlated-noise Gaussian environment. Suppose that Charlie has an entanglement source described by an EPR state ρ_{AB} with CM $\mathbf{V}_{AB}(\mu)$ given in Eq. (33). We consider the different scenarios depicted in the two panels of Fig. 5. Charlie may attempt to distribute entanglement to Alice and Bob as shown in the left panel of Fig. 5, or he may try to share entanglement with one of the remote parties, e.g., Bob, as shown in the right panel of Fig. 5 (by symmetry, our derivation is the same if we consider Alice in the place of Bob).

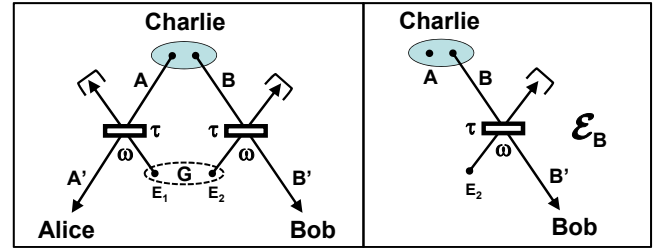


FIG. 5: Scenarios for entanglement distribution. *Left.* Charlie has two modes A and B prepared in an EPR state ρ_{AB} . In order to distribute entanglement to the remote parties, Charlie transmits the two modes through the correlated Gaussian environment, characterized by transmissivity τ , thermal noise ω and correlations \mathbf{G} . *Right.* Charlie aims to share entanglement with a remote party (e.g., Bob). He then keeps mode A while sending mode B through the lossy channel \mathcal{E}_B .

Let us start from the scenario where Charlie aims to share entanglement with Bob, which means that he keeps mode A while sending mode B . The action of the environment is therefore reduced to $\mathcal{I}_A \otimes \mathcal{E}_B$, where \mathcal{E}_B is a lossy channel with transmissivity τ and thermal noise ω . It is easy to check [33] that the output state $\rho_{AB'}$, shared by Charlie and Bob, is Gaussian with zero mean and CM

$$\mathbf{V}_{AB'} = \begin{pmatrix} \mu \mathbf{I} & \mu' \sqrt{\tau} \mathbf{Z} \\ \mu' \sqrt{\tau} \mathbf{Z} & x \mathbf{I} \end{pmatrix}, \quad (62)$$

where

$$x := \tau\mu + (1 - \tau)\omega. \quad (63)$$

We can compute closed analytical formulas in the limit of large μ , i.e., large input entanglement. In this case,

the entanglement of the output state $\rho_{AB'}$ is quantified by the PTS eigenvalue

$$\varepsilon = \frac{1 - \tau}{1 + \tau} \omega . \quad (64)$$

The entanglement-breaking condition corresponds to the separability condition $\varepsilon \geq 1$, which provides

$$\omega \geq \frac{1 + \tau}{1 - \tau} := \omega_{\text{EB}} , \quad (65)$$

or, equivalently, $\bar{n} \geq \tau/(1 - \tau)$ for the mean number of thermal photons.

Despite the entanglement-breaking condition of Eq. (65) being derived for an EPR input, it is indeed valid for any input state. In other words, a lossy channel \mathcal{E}_B with transmissivity τ and thermal noise $\omega \geq \omega_{\text{EB}}$ destroys the entanglement of any input state ρ_{AB} . As one can check, Eq. (65) corresponds exactly to the entanglement-breaking condition for lossy channels derived in Ref. [11]. In particular, the threshold condition $\omega = \omega_{\text{EB}}$ is sufficient to guarantee one-mode entanglement-breaking, i.e., the impossibility for Charlie to share any entanglement with a remote party.

Now remember our main question: Suppose that Charlie cannot share any entanglement with Alice or Bob (one-mode entanglement-breaking), can he still distribute entanglement to them? In other words, suppose that the correlated-noise Gaussian environment has transmissivity τ and thermal noise $\omega = \omega_{\text{EB}}$, so that the individual lossy channels \mathcal{E}_A (Charlie→Alice) and \mathcal{E}_B (Charlie→Bob) are entanglement-breaking. Is it still possible to use the joint channel \mathcal{E}_{AB} to distribute entanglement to the remote parties? In the following, we explicitly reply to this question. In particular, we will show that entanglement can be distributed by separable environments and can be large enough to be distilled by one-way distillation protocols.

Let us derive the general evolution of the two modes A and B under the action of the joint environment, as depicted in the left panel of Fig. 5. Since the input EPR state ρ_{AB} is Gaussian and the environmental state $\rho_{E_1 E_2}$ is Gaussian, the output state $\rho_{A'B'}$ is also Gaussian. This state has zero mean and CM given by

$$\mathbf{V}_{A'B'} = \tau \mathbf{V}_{AB} + (1 - \tau) \mathbf{V}_{E_1 E_2} = \begin{pmatrix} x\mathbf{I} & \mathbf{H} \\ \mathbf{H} & x\mathbf{I} \end{pmatrix} , \quad (66)$$

where

$$\mathbf{H} := \tau \mu' \mathbf{Z} + (1 - \tau) \mathbf{G} . \quad (67)$$

For large input entanglement $\mu \gg 1$, we can easily derive the symplectic spectrum of the output state

$$\nu_{\pm} = \sqrt{(2\omega + g' - g \pm |g + g'|)(1 - \tau)\tau\mu} , \quad (68)$$

and its smallest PTS eigenvalue

$$\varepsilon = (1 - \tau) \sqrt{(\omega - g)(\omega + g')} . \quad (69)$$

The latter eigenvalue determines the remote entanglement distributed to Alice and Bob, equivalently quantified by the log-negativity

$$\mathcal{N} = \max\{0, -\log \varepsilon\} , \quad (70)$$

which is measured in entanglement bits (ebits). In particular, \mathcal{N} represents an upper bound to the mean number of ebits which are distillable per output copy $\rho_{A'B'}$.

In the same limit, we can also compute the coherent information $I(A)B$ between the two remote parties, which provides a lower bound to the mean number of ebits per copy that can be distilled using one-way distillation protocols, i.e., protocols based on local operations and one-way classical communication (see Appendix B3 for more details). This is clearly a lower bound since one-way distillability implies two-way distillability, where both forward and backward communication are generally exploited. In the remainder of the paper, by distillability we implicitly mean the sufficient condition of one-way distillability.

For large input entanglement $\mu \gg 1$, we can write

$$I(A)B = -\log(\varepsilon\varepsilon) , \quad (71)$$

which is derived by expanding the coherent information for diverging spectra (see Appendix B3). Thus, remote entanglement is distributed for $\varepsilon < 1$, according to Eq. (70), and it is furthermore distillable for $\varepsilon < e^{-1}$, according to Eq. (71).

Now suppose that the Gaussian environment has thermal noise $\omega = \omega_{\text{EB}}$, so that it is one-mode entanglement-breaking. Replacing in Eq. (69), we can write

$$\begin{aligned} \varepsilon &= \sqrt{[1 + \tau - (1 - \tau)g][1 + \tau + (1 - \tau)g']} \\ &:= \varepsilon(\tau, g, g') \end{aligned} \quad (72)$$

Answering our previous question corresponds to finding environmental parameters τ , g and g' , for which ε is sufficiently low: For a given value of the transmissivity τ , we look for regions in the correlation plan (g, g') where $\varepsilon < 1$ (remote entanglement is distributed) and, more strongly, $\varepsilon < e^{-1}$ (remote entanglement is distillable). This is done in Fig. 6 for several numerical values of the transmissivity.

In Fig. 6, the environments identified by the gray “reactivation area” allow Charlie to distribute entanglement to Alice and Bob ($\varepsilon < 1$), despite being impossible for him to share any entanglement with the remote parties. In other words, these environments allow two-mode entanglement-distribution, despite being one-mode entanglement-breaking. Furthermore, we can identify sufficiently-correlated environments for which the entanglement remotely distributed is also distillable ($\varepsilon < e^{-1}$). From Fig. 6, it is evident that entanglement restoration is a threshold process occurring only after a critical amount of correlations is injected by the environment. In particular, the critical values of the correlation parameters, g and g' , correspond to the border of the reactivation area.

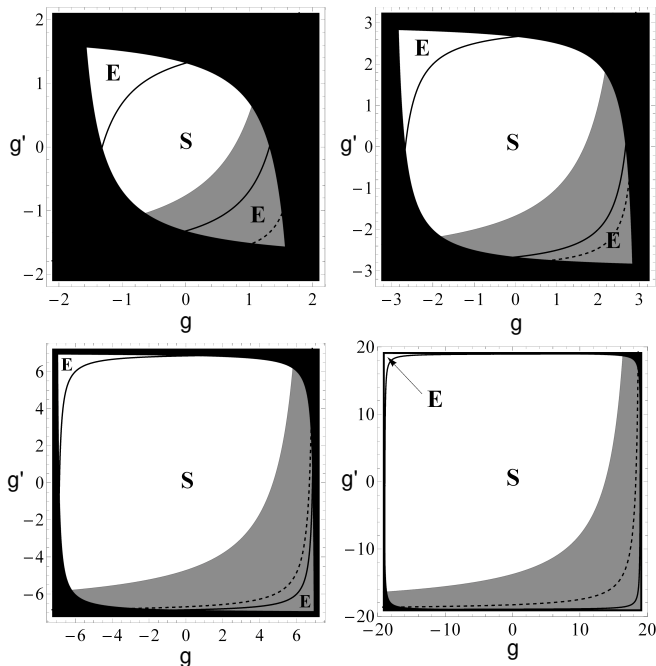


FIG. 6: Analysis of the remote entanglement ε on the correlation plan (g, g') for different values of the transmissivity $\tau = 0.3, 0.5, 0.75,$ and 0.9 (from top left to bottom right). Corresponding values of the thermal noise are determined by the condition of one-mode entanglement-breaking $\omega = \omega_{\text{EB}}$. In each inset, the non-black area identifies the set of physical environments, which are divided into separable (S) and entangled (E) environments by the solid lines. The gray region is the reactivation area and identifies those environments for which Charlie is able to distribute entanglement to Alice and Bob ($\varepsilon < 1$). Within the reactivation area, the points below the dashed curve are those environments for which the distributed entanglement is also distillable ($\varepsilon < e^{-1}$).

The most remarkable feature in Fig. 6 is represented by the presence of separable environments in the reactivation area. In other words, there are separable Gaussian environments which contain enough correlations to restore the distribution of entanglement to Alice and Bob. Furthermore, for sufficiently-high transmissivities and correlations, these environments enable Charlie to distribute a distillable amount of entanglement. For instance, see the bottom right panel of Fig. 6, where separable environments are predominant.

Thus, we have just proven that a distillable fraction of the large input entanglement can be remotely restored by the presence of separable correlations in the Gaussian environment, which are therefore sufficiently strong to break the mechanism of entanglement-breaking induced by the thermal noise. As we have already said, achieving the simultaneous conditions of one-mode entanglement-breaking and two-mode entanglement-distribution is here surprising, since there is no decoherence-free subspace which can preserve the input entanglement and there is no entanglement coming from the environment which can replace the amount lost in the transmission.

By contrast, the conditions of one-mode entanglement-breaking and two-mode entanglement-distribution can be trivially achieved in entangled environments. For instance, we may consider two beam-splitters with zero transmissivity, so that Charlie's state is completely reflected into the environment and the entangled state of the environment is reflected to Alice and Bob. This scenario is certainly one-mode entanglement-breaking, since Charlie has no chance of sharing part of his state with Alice or Bob. At the same time, two-mode entanglement-distribution is realized, since the loss of Charlie's initial entanglement is just replaced by the injection of entanglement from the environment.

1. Distribution and distillation in SC environments

Here we specify the previous analysis to SC environments ($g' = g$). We consider these separable environments at the thermal threshold $\omega = \omega_{\text{EB}}$, so that they are one-mode entanglement-breaking. In the limit of large μ , we derive the parameter regimes for which remote entanglement can be distributed by the two-mode transmission and, more strongly, result into distillable entanglement. In particular, we provide simple threshold conditions for the correlation parameter g . Finally, we study the relations between remote entanglement and the various types of separable correlations (quantum and classical) present in these environments, quantifying the critical number of correlation bits which are needed for entanglement restoration.

From Eq. (72), we see that Alice and Bob's remote entanglement can be quantified by

$$\varepsilon_{\text{SC}} = \varepsilon(\tau, g, g) = \sqrt{(1 + \tau)^2 - (1 - \tau)^2 g^2}. \quad (73)$$

Since ε_{SC} does not depend on the sign of g , its study can be reduced to SC environments with positive g . It is easy to check that ε_{SC} takes its optimal (minimum) value

$$\varepsilon_{\text{MSC}} = \sqrt{(1 - \tau)(1 + 3\tau)}, \quad (74)$$

when the environment has maximal correlations (MSC environment), with correlation parameter

$$g_{\text{MSC}} = \omega_{\text{EB}} - 1 = \frac{2\tau}{1 - \tau}. \quad (75)$$

From Eq. (73), we can see that remote entanglement is restored ($\varepsilon_{\text{SC}} < 1$) for transmissivities $\tau > 2/3$ and values of the correlation parameter $g_{\text{ER}} < g \leq g_{\text{MSC}}$, where g_{ER} is the entanglement-restoration threshold

$$g_{\text{ER}} = \frac{\sqrt{\tau(\tau + 2)}}{1 - \tau}. \quad (76)$$

More strongly, remote entanglement is distillable ($\varepsilon_{\text{SC}} < e^{-1}$) for $\tau \gtrsim 0.96$ and $g_{\text{ED}} < g \leq g_{\text{MSC}}$, where g_{ED} is the entanglement-distillation threshold

$$g_{\text{ED}} := \frac{\sqrt{e^2(1 + \tau)^2 - 1}}{e(1 - \tau)} \geq g_{\text{ER}}. \quad (77)$$

See Fig. 7 for a pictorial representation.

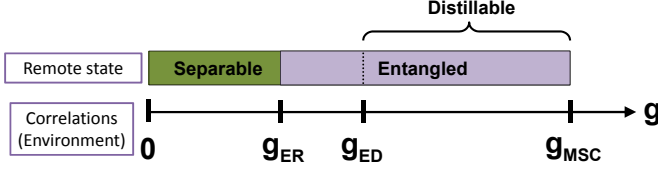


FIG. 7: Scheme showing the separability properties of Alice and Bob's remote state in terms of the correlation parameter g of the SC environment (which is always separable). Here we consider the regime of high transmissivity $\tau \gtrsim 0.96$, where remote entanglement can be distilled for sufficiently high values of the correlation parameter ($g > g_{ED}$).

As discussed in Sec. III A 2, we can easily quantify the separable correlations of the SC environments in terms of classical correlations C and Gaussian discord D . These environmental quantities can be connected with the amount of entanglement which is restored at the remote stations under the usual conditions one-mode entanglement-breaking ($\omega = \omega_{EB}$) and large input entanglement ($\mu \gg 1$). As we can see from the top panel of Fig. 8, remote entanglement can be restored ($\varepsilon_{SC} < 1$) only after a certain amount of Gaussian discord D and classical correlations C . Plot refers to the numerical case of $\tau = 0.9$, but the same behavior appears for any other value of transmissivity $\tau > 2/3$.

In the bottom panel of Fig. 8, we have plotted the number of ebits remotely restored (as quantified by the log-negativity \mathcal{N}) versus the environmental Gaussian discord D (solid line) and classical correlations C (dashed line). We can clearly see the threshold behavior of the entanglement, which starts to be restored only after a certain numbers of correlation bits (dbits and cbits) are injected by the environment. After these critical values, the number of remote ebits is monotonically increasing.

Entanglement restoration is a threshold process at any transmissivity $\tau > 2/3$. This is particularly evident from Fig. 9, where we plot the critical numbers of dbits and cbits, after which remote entanglement is established. For completeness, we also plot the critical number of bits of total correlations (quantified by the quantum mutual information) which are needed for the restoration. As we can see, we need less than 2 bits of total correlations to recover entanglement at any $\tau > 2/3$. Also note that, for extremely low loss ($\tau \rightarrow 1$) and high thermal noise ($\omega_{EB} \rightarrow +\infty$), restoration is achieved in correspondence of a negligible amount of Gaussian discord and 2 bits of classical correlations.

2. Distribution and distillation in AC environments

Here we repeat the previous analysis for the case of AC environments ($g' = -g$), under the same conditions of one-mode entanglement-breaking ($\omega = \omega_{EB}$) and large input entanglement ($\mu \gg 1$). Using Eq. (72), we see that

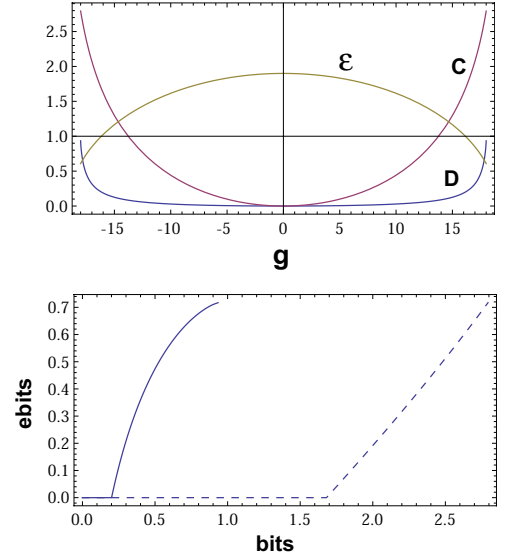


FIG. 8: *Top panel.* PTS eigenvalue ε_{SC} (dimensionless units), Gaussian discord D (dbits) and classical correlations C (cbits) are plotted versus the correlation parameter g of the SC environment (note that we can restrict our analysis to $g > 0$ by symmetry). Remote entanglement is generated ($\varepsilon_{SC} < 1$) for sufficiently high values of D and C , and it is optimal at the border (MSC environments), where D and C are maximal. In this numerical example, transmission is $\tau = 0.9$ and thermal noise is $\omega = \omega_{EB} = 19$ (one-mode entanglement-breaking). *Bottom panel.* Remote entanglement, as quantified by the log-negativity (ebits), is plotted versus the Gaussian discord (dbits, solid line) and the classical correlations (cbits, dashed line). Remote entanglement starts to be restored only after a critical number of correlation bits are injected. Then, it is monotonically increasing. Numerical parameters are identical as before ($\tau = 0.9$ and $\omega = 19$).

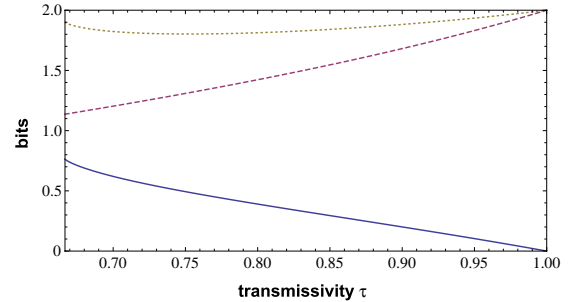


FIG. 9: For SC environments at any transmissivity $\tau > 2/3$, we plot the critical number of correlation bits after which remote entanglement starts to be restored. We show the critical number of dbits (solid), cbits (dashed) and their total (dotted), corresponding to bits of quantum mutual information.

Alice and Bob's remote entanglement is quantified by

$$\varepsilon_{AC} = \varepsilon(\tau, g, -g) = 1 + \tau - (1 - \tau)g. \quad (78)$$

We can have $\varepsilon_{AC} < 1$ only for positive values of the correlation parameter g . Such an asymmetry, which is also evident from Fig. 6, depends on the fact that Charlie's input state has EPR correlations of the type $\hat{q}_A \simeq \hat{q}_B$ and

$\hat{p}_A \simeq -\hat{p}_B$. These input correlations tend to be preserved by AC environments with positive g (whose correlations are of the same type) while they tend to be destroyed by AC environments with negative g (opposite type).

For this reason, in our analysis we only consider positive AC environments ($g > 0$) which are separable for $g \leq g_{\text{MAC}} = \omega_{\text{EB}} - 1$, and entangled for

$$g_{\text{MAC}} < g \leq g_{\text{EPR}} = \sqrt{\omega_{\text{EB}}^2 - 1} = \frac{2\sqrt{\tau}}{1-\tau}. \quad (79)$$

The optimal restoration of entanglement is achieved by the positive EPR environment $g = g_{\text{EPR}}$, for which we have $\varepsilon_{\text{EPR}} = (1 - \sqrt{\tau})^2$. One can easily check that this is the global optimum in the entire correlation plan. Optimal restoration in separable AC environments is achieved by the positive MAC environment ($g = g_{\text{MAC}}$) for which

$$\varepsilon_{\text{MAC}} = 1 - \tau. \quad (80)$$

In general, from Eq. (78), we see that remote entanglement is restored at any transmissivity τ for values of the correlation parameter $g_{\text{ER}} < g \leq g_{\text{EPR}}$, where the entanglement-restoration threshold is here equal to

$$g_{\text{ER}} := \frac{\tau}{1-\tau}. \quad (81)$$

This threshold satisfies $g_{\text{ER}} = g_{\text{MAC}}/2$, which means that remote entanglement can always be recovered by separable AC environments with sufficiently high correlations, as pictorially shown in Fig. 10.

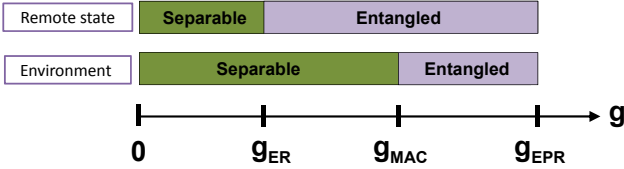


FIG. 10: Separability properties of the remote state versus those of the positive AC environments ($g > 0$). For $g_{\text{ER}} < g \leq g_{\text{MAC}}$, there are separable AC environments able to restore remote entanglement.

Thus, at any transmissivity τ , there always exist separable AC environments able to reactivate the entanglement distribution. In particular, this is true for $\tau \simeq 0$ (and therefore $\omega_{\text{EB}} \simeq 1$). In fact, by expanding at the leading order in τ , we get

$$g_{\text{ER}} \simeq \tau, \quad g_{\text{MAC}} \simeq 2\tau, \quad g_{\text{EPR}} \simeq 2\sqrt{\tau}, \quad (82)$$

which means that we can always find a correlation parameter $g \simeq 0$ such that $g_{\text{ER}} < g \leq g_{\text{MAC}}$. Remarkably, in conditions of extreme losses, where entanglement is broken by a negligible amount of thermal noise, entanglement distribution can be reactivated by a vanishing amount of separable correlations ($g_{\text{ER}} \simeq \tau \simeq 0$).

Proceeding with our analysis of the AC environments, we see that entanglement distillation is possible for transmissivities

$$\tau > e^{-1}(\sqrt{e} - 1)^2 \simeq 0.15, \quad (83)$$

and values of the correlation parameter $g_{\text{ED}} < g \leq g_{\text{EPR}}$, where the entanglement-distillation threshold is now

$$g_{\text{ED}} := \frac{1 + \tau - e^{-1}}{1 - \tau} \geq g_{\text{ER}}. \quad (84)$$

At high transmissivities $\tau > 1 - e^{-1} \simeq 0.63$, we have $g_{\text{ED}} < g_{\text{MAC}}$, which means that distillable entanglement can be restored in the presence of separable AC environments. For a pictorial representation see Fig. 11.

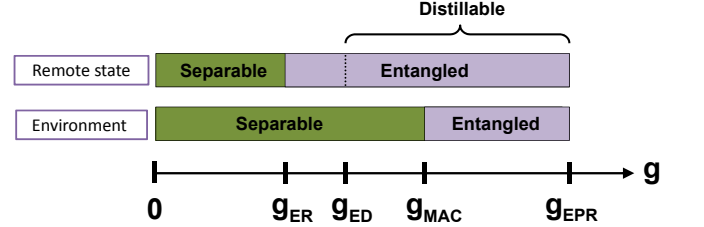


FIG. 11: Separability properties of the remote state versus those of the positive AC environments ($g > 0$). Here we consider the regime of high transmissivity $\tau \gtrsim 0.63$, where remote entanglement can be distilled even in the presence of separable environments ($g_{\text{ED}} < g \leq g_{\text{MAC}}$).

Finally, we analyze the behavior of the remote entanglement in terms of the different types of environmental correlations. As evident from the top panel of Fig. 12, remote entanglement starts to be restored ($\varepsilon_{\text{AC}} < 1$) only after certain values of Gaussian discord and classical correlations are present in the positive AC environment. After these critical values, the number of remote ebits of log-negativity are increasing in both correlations, as shown in the bottom panel of Fig. 12. Curves refer to the same numerical example as before ($\tau = 0.9$) and similar behavior holds at other transmissivities. In general, the positive AC environments outperform the SC environments in restoring entanglement, as it is clear by comparing the curves of Fig. 12 to those of Fig. 8. Such a better performance can also be recognized from the asymmetric shape of the reactivation area in Fig. 6.

The better performance of these environments is also evident from Fig. 13, where we plot the critical number of correlation bits which are needed for the restoration of remote entanglement (dbits, cbits and bits of total correlations). We need less than $2 - \log 3 \simeq 0.415$ bits of total correlations to trigger the reactivation at any transmissivity τ . In particular, the critical number of dbits is always less than 0.05. For τ close to zero, a negligible amount of correlations is needed. This is compatible with the fact that, for these environments, the threshold for entanglement-restoration g_{ER} goes rapidly to zero for $\tau \rightarrow 0$, so that a small $g > g_{\text{ER}} \simeq 0$ is sufficient to reactivate the entanglement distribution in the high loss regime. In the opposite regime of extremely low loss ($\tau \rightarrow 1$) and high thermal noise ($\omega_{\text{EB}} \rightarrow +\infty$), the critical number of dbits falls to zero while the numbers of cbits tend to its maximum.

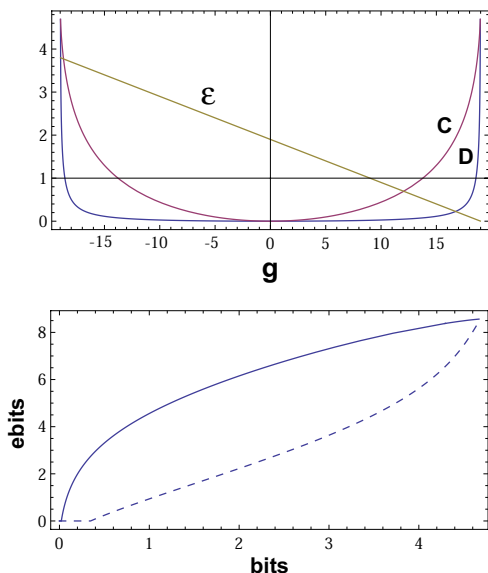


FIG. 12: *Top panel.* PTS eigenvalue ε_{AC} (dimensionless units), Gaussian quantum discord D (dbits) and purely-classical correlations C (cbits) are plotted versus the correlation parameter g of the AC environment. Remote entanglement is restored ($\varepsilon_{AC} < 1$) only in positive AC environments ($g > 0$) and after critical values of D and C . Optimal restoration is achieved for the positive EPR environment, where $C = D$ are maximal. Numerical example for $\tau = 0.9$ and $\omega = \omega_{EB} = 19$. *Bottom panel.* Remote entanglement quantified by the log-negativity (ebits) is plotted versus Gaussian discord (dbits, solid line) and classical correlations (cbits, dashed line) present in the environment. Once entanglement is reactivated, the number of remote ebits is increasing in the number of environmental dbits and cbits (here τ and ω are chosen as before).

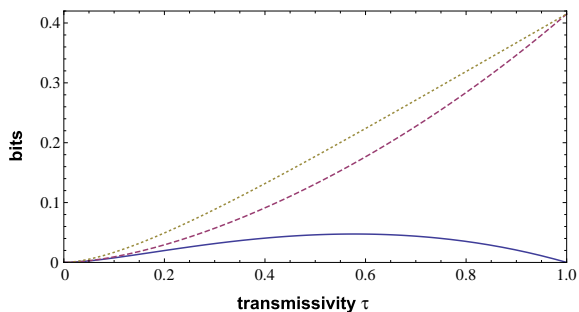


FIG. 13: For positive AC environments at any τ , we plot the critical number of correlation bits after which remote entanglement starts to be restored. We show the critical numbers of dbits (solid), cbits (dashed) and their total (dotted), corresponding to bits of quantum mutual information.

3. General non-monotonicity of entanglement restoration

According to the previous sections, the restoration of entanglement is a threshold process which starts only after a critical amount of environmental correlations is injected into the travelling modes. After this threshold, the number of ebits remotely recovered is monotonically

increasing in the number of correlation bits (dbits, cbits or total bits). However, this monotonic behavior holds true as long as we compare environments within the same class, i.e., we analyze SC environments separately from AC environments. In general, the monotonicity is lost when we compare two arbitrary points in the correlation plan. For instance, it is sufficient to compare the MSC environment with the (positive) MAC environment to find that entanglement restoration is not monotonic in any type of correlations, i.e., classical, quantum or total.

As we have already discussed in Sec. III A 2, at any fixed thermal noise $\omega > 1$, MSC and MAC environments have exactly the same amount of classical correlations $C_{MSC} = C_{MAC}$, but different Gaussian discord $D_{MSC} > D_{MAC}$ and, therefore, different total correlations $I_{MSC} > I_{MAC}$. This is because MAC environments are more entropic than MSC environments. Their difference in entropy

$$\delta S := S_{MSC} - S_{MAC} = h(2\omega - 1) - 2h(\sqrt{2\omega - 1}) < 0, \quad (85)$$

directly quantifies the difference in the correlations, i.e.,

$$D_{MSC} - D_{MAC} = I_{MSC} - I_{MAC} = -\delta S > 0. \quad (86)$$

In particular, all these relations hold true at the threshold for entanglement-breaking $\omega = \omega_{EB}$, where the number of ebits remotely restored is bigger for the positive MAC environment, i.e., the log-negativities satisfy

$$\mathcal{N}_{MSC} < \mathcal{N}_{MAC}, \quad (87)$$

which is equivalent to $\varepsilon_{MSC} > \varepsilon_{MAC}$, where the two eigenvalues ε_{MSC} and ε_{MAC} are given in Eqs. (74) and (80), respectively. Thus, in this specific example, an increase in the environmental correlations, quantified by the Gaussian discord ($D_{MSC} > D_{MAC}$) or the total correlations ($I_{MSC} > I_{MAC}$), corresponds to a decrease in the number of ebits remotely recovered ($\mathcal{N}_{MSC} < \mathcal{N}_{MAC}$). At the same time, we also see that this decrease happens for constant classical correlations ($D_{MSC} = D_{MAC}$).

Such a phenomenon could have different potential explanations. There could be a problem with Gaussian discord, which could not be equal to the actual discord for these environments. If this were true, we would have a different quantification for both quantum correlations D and classical correlations C . Then, monotonicity could be re-established in terms of these actual quantities. More drastically, it could be that entanglement restoration might be monotonically connected with a different and more subtle quantification of the environmental correlations.

It is also important to note that this analysis does not change if we consider a different quantification for the remote entanglement. For instance, we could consider the entanglement of formation [76] in the place of the log-negativity to quantify the entanglement of Alice and Bob's two-mode state. However, such a state turns out to be a symmetric Gaussian state, so that its entanglement of formation is equal to its Gaussian entanglement

of formation [77], which is monotonically related to its log-negativity [78].

4. Evolution of the EPR correlations

In order to give another point of view to the dynamics of the process, we describe the evolution of the EPR correlations of Charlie's input state when the two modes are transmitted through the correlated-noise Gaussian environment, with transmission τ , thermal noise ω and correlations \mathbf{G} , as depicted in the left panel of Fig. 5 (see Appendix B 4 for more details on EPR correlations). As we will see below, the entanglement restored at Alice's and Bob's stations is not necessarily in the form EPR correlations.

We can easily write the input-output Bogoliubov transformations for the bosonic modes involved in the process

$$\hat{\mathbf{x}}_{A'} = \sqrt{\tau}\hat{\mathbf{x}}_A + \sqrt{1-\tau}\hat{\mathbf{x}}_{E_1} \quad (88)$$

$$\hat{\mathbf{x}}_{B'} = \sqrt{\tau}\hat{\mathbf{x}}_B + \sqrt{1-\tau}\hat{\mathbf{x}}_{E_2} \quad (89)$$

where $\hat{\mathbf{x}} = (\hat{q}, \hat{p})^T$ is a vector of quadratures. From these equations, we can extract the output EPR operators

$$\hat{q}'_- := \frac{\hat{q}_{A'} - \hat{q}_{B'}}{\sqrt{2}}, \quad \hat{p}'_+ := \frac{\hat{p}_{A'} + \hat{p}_{B'}}{\sqrt{2}}. \quad (90)$$

Now, using the CM of the input EPR state (33) and that of the environment (38), we can compute their variances

$$\begin{aligned} \mathbf{\Lambda} &:= \begin{pmatrix} V(\hat{q}'_-) & \\ & V(\hat{p}'_+) \end{pmatrix} \\ &= \tau(\mu - \mu')\mathbf{I} + (1-\tau)(\omega\mathbf{I} - \mathbf{ZG}). \end{aligned} \quad (91)$$

In the limit of $\mu \gg 1$, we have

$$\mathbf{\Lambda} \rightarrow \mathbf{\Lambda}_\infty = (1-\tau)(\omega\mathbf{I} - \mathbf{ZG}), \quad (92)$$

and assuming entanglement-breaking ($\omega = \omega_{\text{EB}}$) we get

$$\mathbf{\Lambda}_{\infty, \text{EB}} = (1+\tau)\mathbf{I} - (1-\tau)\mathbf{ZG}. \quad (93)$$

Analyzing Eq. (93) we see that the EPR condition $\mathbf{\Lambda}_{\infty, \text{EB}} < \mathbf{I}$ can be realized by suitable choices of the correlation block \mathbf{G} (here the EPR condition corresponds to having quadrature correlations between the output modes, quantified by the variances $V(\hat{q}'_-)$ and $V(\hat{p}'_+)$, which are below the unit-variance of the vacuum noise).

Let us explicitly compare the different types of environments. For the memoryless environment ($\mathbf{G} = \mathbf{0}$) we have $\mathbf{\Lambda}_{\infty, \text{EB}} = (1+\tau)\mathbf{I}$ which means that the EPR variances are always greater than or equal to one, i.e., EPR correlations do not survive.

For the AC environment ($\mathbf{G} = g\mathbf{Z}$) we have

$$\mathbf{\Lambda}_{\infty, \text{EB}} = [(1+\tau) - (1-\tau)g]\mathbf{I}. \quad (94)$$

It is easy to check that the EPR condition $\mathbf{\Lambda}_{\infty, \text{EB}} < \mathbf{I}$ is achieved by physical values of $g > g_{\text{ER}}$, where g_{ER} is

given in Eq. (81). This means that the remote entanglement generated by this environment is always in the form of EPR correlations (of the same type of the original EPR state at Charlie's station).

For the SC environment ($\mathbf{G} = g\mathbf{I}$) we have

$$\mathbf{\Lambda}_{\infty, \text{EB}} = (1+\tau)\mathbf{I} - (1-\tau)g\mathbf{Z}, \quad (95)$$

and we can check that the condition $\mathbf{\Lambda}_{\infty, \text{EB}} < \mathbf{I}$ is not realizable by any choice of g . Thus, the initial EPR correlations do not survive in this case. Nevertheless we have explicitly proven that remote entanglement can be distributed in the presence of this environment.

IV. CONCLUSION AND DISCUSSION

In conclusion, we have shown how the combination of two entanglement-breaking channels into a joint correlated-noise environment can restore the distribution of entanglement. Interestingly, this reactivation is successfully induced by the presence of separable correlations and occurs for quantum systems with Hilbert spaces of any dimension (qubits, qudits and bosonic modes).

In our first analysis, we have considered twirling environments which are classically-correlated, being realizable by random LOCCs and described by zero-discord environmental states. We have considered correlated Pauli environments for qubits, multidimensional twirling environments for qudits and, finally, non-Gaussian bosonic environments based on phase-space rotations. All these scenarios are characterized by one-system entanglement-breaking (so that Charlie cannot share any entanglement with Alice or Bob), and two-system entanglement-preserving (so that Charlie is able to transmit entanglement to Alice and Bob).

Achieving these simultaneous conditions is somehow easy for these environments, since there are well-known classes of entangled states which are invariant under their action (thus forming decoherence-free subspaces). Depending on the type of twirling, i.e., $U \otimes U$ or $U \otimes U^*$, these invariant states are Werner or isotropic states, respectively. In the case of bosonic systems, we can find entangled states which are invariant under the action of anti-correlated phase-space rotations $R_\theta \otimes R_{-\theta}$, and they coincide with the continuous-variable Werner states.

More interestingly, in our second analysis on bosonic systems in Gaussian environments, we have shown how entanglement distribution is still possible even in the absence of decoherence-free subspaces (a similar relaxation of conditions can also be found in the context of quantum error correction [79]). In this case, entanglement is no longer preserved but still can survive the double transmission and be distilled by the remote parties.

More precisely, we have considered a realistic model of Gaussian environment with correlated noise, which generalizes the standard memoryless environment with losses and thermal noise. Then, we have imposed the condition

of one-mode entanglement-breaking by choosing a sufficiently high value of thermal noise ω_{EB} for any value of the transmission (so that Charlie can never share entanglement with the remote parties). Under these conditions of extreme decoherence, we have shown that a distillable amount of entanglement is able to survive the two-mode transmission and reach Alice's and Bob's stations. This reactivation of entanglement distribution is a direct effect of the correlations which are injected by the Gaussian environment. Remarkably, the injection of separable correlations is sufficient to break the mechanism of entanglement-breaking and trigger the reactivation.

In a further analysis, we have shown that remote entanglement starts to be restored only after a critical amount of correlations is present in the environment, where these correlations can be quantified in terms of Gaussian discord, classical correlations and total correlations (quantum mutual information). After this critical amount has been reached, the number of remote ebits is not always increasing in the number of correlation bits injected by the environment, despite such a monotonicity being true when we restrict the environments to classes with specific types of noise correlations (SC and AC environments). It is possible that the monotonicity could be extended to the entire correlation plan if Gaussian discord were proven to be strictly larger than the actual discord. More drastically, the monotonicity could hold in terms of a different and unknown quantification of the environmental correlations.

From a theoretical point of view, the fact that separability can be exploited to recover from entanglement-breaking is a paradoxical behavior which poses fundamental questions on the intimate relations between local and nonlocal correlations. While the reactivation process is easily understandable in the presence of entangled environments, where the original system entanglement is partly or fully replaced by the environmental entanglement, its interpretation is puzzling in the case of separable environments, where no injection of entanglement may take place.

In conclusion, in terms of potential practical impact, our analysis shows new perspectives for entanglement distribution and distillation in conditions of extreme decoherence as long as the presence of noise correlations and memory effects can be identified in the environment, such as those arising from non-Markovian dynamics of open quantum systems [16, 17]. According to our findings, such correlations and effects do not need to be strong, since separable correlations and classical memories may be sufficient to restore broken entanglement.

Note that memory channels and non-Markovian environments are ubiquitous. For instance, they naturally arise in the context of spin chains [23] and micro-masers [24]. Other important examples can be found in condensed matter, in particular when we consider the dynamics of quantum dots in photonic crystals [25]. In the bosonic setting, memory Gaussian channels come into play when electromagnetic modes propagate through

dispersive media, such as linear optical systems or free-space. In this case, correlations and memory effects are naturally introduced by diffraction [26–29]. Finally, other examples of bosonic memory channels can also be found in the propagation of electromagnetic radiation through atmospheric turbulence [30–32].

V. ACKNOWLEDGEMENTS

This work has been supported by EPSRC under the research grant HIPERCOM (EP/J00796X/1) and by The Leverhulme Trust. Special thanks of the author are for S. L. Braunstein, M. Paternostro and C. Ottaviani. The author would also like to thank (in random order) P. Horodecki, O. Oreshkov, A. Furusawa, G. Spedalieri, G. Adesso, M. Gu, S. Mancini, G. Chiribella, O. Hirota, B. Munro, N. Metwally, R. Namiki, P. Tombesi, S. Guha, M. J. W. Hall, S. Danilishin, M. Barbieri, M. Bellini, R. Filip, and J. Eschner for discussions and comments.

Appendix A: Miscellaneous proofs

Here we report some of the proofs related to our analysis of entanglement preservation in twirling environments. This appendix contains new results but also known facts which are given to the reader for the sake of completeness (e.g., Sec. A 4).

1. Entanglement-breaking conditions for qubit depolarizing channels

Here we show the conditions under which the depolarizing channel of Eq. (8) becomes an entanglement-breaking channel. This means to find a specific regime for the probabilities $\{p_k\}_{k=0}^3$ characterizing the channel.

First of all note that, for Hilbert spaces of finite dimension d , a simple way to check if a quantum channel \mathcal{E} is entanglement-breaking is to test it on the maximally-entangled state $|\psi\rangle_{AB}$ of Eq. (22). In other words, if $(\mathcal{E}_A \otimes \mathcal{I}_B)|\psi\rangle_{AB}$ is separable, then $(\mathcal{E}_A \otimes \mathcal{I}_B)\rho_{AB}$ is separable for any input state ρ_{AB} [10]. In the case of qubits, we can test the channel on the triplet state $|+\rangle_{AB}$ of Eq. (23). We then compute the output state

$$\begin{aligned} \Phi &:= (\mathcal{E}_A \otimes \mathcal{I}_B)(|+\rangle_{AB} \langle +|) \\ &= \sum_{k=0}^3 p_k (P_k \otimes I) |+\rangle_{AB} \langle +| (P_k^\dagger \otimes I) \\ &= p_0 |+\rangle_{AB} \langle +| \\ &+ p_1 (X \otimes I) |+\rangle_{AB} \langle +| (X \otimes I) \\ &+ p_2 (Y \otimes I) |+\rangle_{AB} \langle +| (Y^\dagger \otimes I) \\ &+ p_3 (Z \otimes I) |+\rangle_{AB} \langle +| (Z \otimes I). \end{aligned} \tag{A1}$$

$$\tag{A2}$$

Adopting the computational basis $\{|00\rangle, |01\rangle, |10\rangle, |11\rangle\}$ and using $X|u\rangle = |u \oplus 1\rangle$, $Z|u\rangle = (-1)^u|u\rangle$ and $Y = iXZ$, we get

$$\Phi = \sum_{ijkl} \Phi_{ijkl} |i, j\rangle_{AB} \langle k, l|, \quad (\text{A3})$$

where the coefficients $\Phi_{ijkl} = \langle i, j|\Phi|k, l\rangle$ are the elements of the following density matrix

$$\Phi = \frac{1}{2} \begin{pmatrix} p_0 + p_3 & 0 & 0 & p_0 - p_3 \\ 0 & p_1 + p_2 & p_1 - p_2 & 0 \\ 0 & p_1 - p_2 & p_1 + p_2 & 0 \\ p_0 - p_3 & 0 & 0 & p_0 + p_3 \end{pmatrix}. \quad (\text{A4})$$

To check the separability properties we adopt the Peres-Horodecki criterion [67, 68]. This corresponds to compute the partial transpose (PT) of the state which is given by the following linear map

$$\begin{aligned} \Phi &= \sum_{ijkl} \Phi_{ijkl} |i\rangle_A \langle k| \otimes |j\rangle_B \langle l| \\ &\rightarrow \text{PT}(\Phi) = \sum_{ijkl} \Phi_{ijkl} |i\rangle_A \langle k| \otimes (|j\rangle_B \langle l|)^T \\ &= \sum_{ijkl} \Phi_{ijkl} |i\rangle_A \langle k| \otimes |l\rangle_B \langle j| \\ &= \sum_{ijkl} \Phi_{ilkj} |i\rangle_A \langle k| \otimes |j\rangle_B \langle l|. \end{aligned} \quad (\text{A5})$$

At the level of the density matrix we then have

$$\Phi = ((\Phi_{ijkl})) \rightarrow \text{PT}(\Phi) = ((\Phi_{ilkj})), \quad (\text{A6})$$

i.e., $j \longleftrightarrow l$ swapping. It is easy to check that the partially-transposed matrix

$$\text{PT}(\Phi) = \frac{1}{2} \begin{pmatrix} p_0 + p_3 & 0 & 0 & p_1 - p_2 \\ 0 & p_1 + p_2 & p_0 - p_3 & 0 \\ 0 & p_0 - p_3 & p_1 + p_2 & 0 \\ p_1 - p_2 & 0 & 0 & p_0 + p_3 \end{pmatrix} \quad (\text{A7})$$

has eigenvalues

$$\lambda_k = \frac{1}{2} - p_k \quad (k = 0, 1, 2, 3). \quad (\text{A8})$$

Thus the partially-transposed state has the following spectral decomposition

$$\text{PT}(\Phi) = \sum_{k=0}^3 \left(\frac{1}{2} - p_k \right) |\eta_k\rangle \langle \eta_k|, \quad (\text{A9})$$

with $|\eta_k\rangle$ orthogonal eigenstates. This operator is positive (≥ 0) if and only if

$$p_k \leq \frac{1}{2}, \quad \text{for } k = 0, 1, 2, 3. \quad (\text{A10})$$

As a result, the output state Φ is separable (and the channel is entanglement-breaking) if and only if $p_k \leq 1/2$ for every k , as reported in the main text.

2. Unitary 2-design for the $U \otimes U^*$ twirling channel

Let us consider two qudits with the same dimension d , so that the composite system is described by an Hilbert space $\mathcal{H} = \mathcal{H}_A \otimes \mathcal{H}_B$ with finite dimension d^2 . From the literature [37, 39], we know that we can write the following equality for any input state ρ_{AB} subject to a $U \otimes U$ twirling channel

$$\mathcal{E}_{UU}(\rho_{AB}) := \int_{\mathcal{U}(d)} dU (U \otimes U) \rho_{AB} (U \otimes U)^\dagger \quad (\text{A11})$$

$$= \frac{1}{K} \sum_{k=0}^{K-1} (U_k \otimes U_k) \rho_{AB} (U_k \otimes U_k)^\dagger, \quad (\text{A12})$$

which is valid for $U_k \in \mathcal{D}$, where \mathcal{D} is a unitary 2-design with K elements. Here we can easily show that

$$\mathcal{E}_{UU^*}(\rho_{AB}) := \int_{\mathcal{U}(d)} dU (U \otimes U^*) \rho_{AB} (U \otimes U^*)^\dagger \quad (\text{A13})$$

$$= \frac{1}{K} \sum_{k=0}^{K-1} (U_k \otimes U_k^*) \rho_{AB} (U_k \otimes U_k^*)^\dagger, \quad (\text{A14})$$

where U_k belongs to the same design \mathcal{D} as before. In a few words, the two twirling channels, \mathcal{E}_{UU} and \mathcal{E}_{UU^*} , can be decomposed using the same unitary 2-design.

In the first step of the proof we show that \mathcal{E}_{UU} and \mathcal{E}_{UU^*} are connected by a partial transposition. Consider an arbitrary input state ρ_{AB} decomposed in the orthonormal basis of \mathcal{H} [69]

$$\rho_{AB} = \sum_{ijkl} \rho_{ij}^{kl} |i\rangle_A \langle j| \otimes |k\rangle_B \langle l|. \quad (\text{A15})$$

Its partial transpose corresponds to transposing system B only, i.e.,

$$\text{PT}(\rho_{AB}) = \sum_{ijkl} \rho_{ij}^{kl} |i\rangle_A \langle j| \otimes |l\rangle_B \langle k|. \quad (\text{A16})$$

We first prove that

$$\mathcal{E}_{UU^*}(\rho_{AB}) = \text{PT}\{\mathcal{E}_{UU}[\text{PT}(\rho_{AB})]\}. \quad (\text{A17})$$

In fact, by linearity we have

$$\begin{aligned} \mathcal{E}_{UU}[\text{PT}(\rho_{AB})] &= \int_{\mathcal{U}(d)} dU (U \otimes U) \text{PT}(\rho_{AB}) (U \otimes U)^\dagger \\ &= \sum_{ijkl} \rho_{ij}^{kl} \int_{\mathcal{U}(d)} dU U |i\rangle_A \langle j| U^\dagger \otimes U |l\rangle_B \langle k| U^\dagger. \end{aligned} \quad (\text{A18})$$

Since $[U|l\rangle_B \langle k| U^\dagger]^T = U^* |k\rangle_B \langle l| (U^*)^\dagger$ we get

$$\begin{aligned} &\text{PT}\{\mathcal{E}_{UU}[\text{PT}(\rho_{AB})]\} = \\ &= \sum_{ijkl} \rho_{ij}^{kl} \int_{\mathcal{U}(d)} dU U |i\rangle_A \langle j| U^\dagger \otimes U^* |k\rangle_B \langle l| (U^*)^\dagger \\ &= \int_{\mathcal{U}(d)} dU (U \otimes U^*) \rho_{AB} (U \otimes U^*)^\dagger = \mathcal{E}_{UU^*}(\rho_{AB}). \end{aligned} \quad (\text{A19})$$

Now the second step is to combine Eq. (A17) with the unitary 2-design for \mathcal{E}_{UU} . First it is important to note that the equivalence between Eqs. (A11) and (A12) is valid not only when ρ_{AB} is a density operator but, more generally, when it is an Hermitian linear operator. This extension is straightforward to prove. Suppose that the linear operator $O : \mathcal{H} \rightarrow \mathcal{H}$ is Hermitian. Then its spectral decomposition involves real eigenvalues and orthonormal eigenvectors, i.e., we can write

$$O = \sum_n O_n |\phi_n\rangle \langle \phi_n|, \quad (\text{A20})$$

where $O_n \in \mathbb{R}$ and $\langle \phi_n | \phi_m \rangle = \delta_{nm}$. Now we can write

$$\mathcal{E}_{UU}(O) := \int_{\mathcal{U}(d)} dU (U \otimes U) O (U \otimes U)^\dagger \quad (\text{A21})$$

$$= \sum_n O_n \int_{\mathcal{U}(d)} dU (U \otimes U) |\phi_n\rangle \langle \phi_n| (U \otimes U)^\dagger \quad (\text{A22})$$

$$= \sum_n O_n \frac{1}{K} \sum_{k=0}^{K-1} (U_k \otimes U_k) |\phi_n\rangle \langle \phi_n| (U_k \otimes U_k)^\dagger \quad (\text{A23})$$

$$= \frac{1}{K} \sum_{k=0}^{K-1} (U_k \otimes U_k) O (U_k \otimes U_k)^\dagger, \quad (\text{A24})$$

where (A21)→(A22) by linearity, (A22)→(A23) by the fact that $|\phi_n\rangle \langle \phi_n|$ are projectors (and therefore states) and (A23)→(A24) by linearity again.

As a result, we can apply the equivalence between Eqs. (A21) and (A24) to the linear operator $\text{PT}(\rho_{AB})$ which fails to be a density operator when ρ_{AB} is entangled but still it is Hermitian (and unit trace) in the general case. Thus, we can write

$$\begin{aligned} \mathcal{E}_{UU}[\text{PT}(\rho_{AB})] &= \frac{1}{K} \sum_{t=0}^{K-1} (U_t \otimes U_t) \text{PT}(\rho_{AB}) (U_t \otimes U_t)^\dagger \\ &= \frac{1}{K} \sum_{t=0}^{K-1} \sum_{ijkl} \rho_{ij}^{kl} U_t |i\rangle_A \langle j| U_t^\dagger \otimes U_t |l\rangle_B \langle k| U_t^\dagger. \end{aligned} \quad (\text{A25})$$

Now, using the connection in Eq. (A17) and the fact that $[U_t |l\rangle_B \langle k| U_t^\dagger]^T = U_t^* |k\rangle_B \langle l| (U_t^*)^\dagger$, we can write

$$\begin{aligned} \mathcal{E}_{UU^*}(\rho_{AB}) &= \text{PT}\{\mathcal{E}_{UU}[\text{PT}(\rho_{AB})]\} \\ &= \frac{1}{K} \sum_{t=0}^{K-1} \sum_{ijkl} \rho_{ij}^{kl} U_t |i\rangle_A \langle j| U_t^\dagger \otimes U_t^* |k\rangle_B \langle l| (U_t^*)^\dagger \\ &= \frac{1}{K} \sum_{t=0}^{K-1} (U_t \otimes U_t^*) \rho_{AB} (U_t \otimes U_t^*)^\dagger, \end{aligned} \quad (\text{A26})$$

which gives the equivalence between Eqs. (A13) and (A14).

3. Partial Haar average of a linear operator

In this short appendix we give a simple proof of Eq. (17). Consider an Hilbert space $\mathcal{H} = \mathcal{H}_A \otimes \mathcal{H}_B$ with

finite dimension $d_A d_B$ (where d_A and d_B are generally different). Given a linear operator $T : \mathcal{H} \rightarrow \mathcal{H}$, we can always decompose it in an orthonormal basis

$$T = \sum_{ijkl} T_{ij}^{kl} |i\rangle_A \langle j| \otimes |k\rangle_B \langle l|. \quad (\text{A27})$$

Then, we can write the following partial Haar average, where only system A is averaged on the unitary group

$$\begin{aligned} \langle T \rangle_{U \otimes I} &:= \int_{\mathcal{U}(d)} dU (U \otimes I) T (U^\dagger \otimes I) \\ &= \sum_{ijkl} T_{ij}^{kl} \left(\int_{\mathcal{U}(d)} dU U |i\rangle_A \langle j| U^\dagger \right) \otimes |k\rangle_B \langle l|. \end{aligned} \quad (\text{A28})$$

Now we use Eq. (18) with linear operator $O = |i\rangle_A \langle j|$, which gives

$$\int_{\mathcal{U}(d)} dU U |i\rangle_A \langle j| U^\dagger = \delta_{ij} \frac{I}{d_A}. \quad (\text{A29})$$

Then, by replacing this expression in Eq. (A28), we get

$$\begin{aligned} \langle T \rangle_{U \otimes I} &= \frac{I}{d_A} \otimes \sum_{ikl} T_{ii}^{kl} |k\rangle_B \langle l| \\ &= \frac{I}{d_A} \otimes \text{Tr}_A(T). \end{aligned} \quad (\text{A30})$$

This is a simple extension of Eq. (18) to considering the presence of a second (unaveraged) system B . In particular, for T density operator, we have the result of Eq. (17).

4. Uniformly dephasing channel is entanglement-breaking

Here we prove that the uniformly dephasing channel of Eq. (28) is entanglement-breaking. This is a simple proof of a very intuitive fact, which is given to the reader for completeness. First of all, let us consider a pure input state $\rho_{AB} = |\varphi\rangle_{AB} \langle \varphi|$, expressed in the Fock basis of the two modes as

$$|\varphi\rangle_{AB} = \sum_{kj} c_{kj} |k\rangle_A \otimes |j\rangle_B, \quad \sum_{kj} |c_{kj}|^2 = 1. \quad (\text{A31})$$

Since $R_\theta |k\rangle = \exp(-i\theta k) |k\rangle$, we get

$$\begin{aligned} \rho_{A'B} &= \sum_{kjk'j'} c_{kj} c_{k'j'}^* \left(\int \frac{d\theta}{2\pi} e^{-i\theta(k-k')} |k\rangle_A \langle k'| \right) \otimes |j\rangle_B \langle j'| \\ &= \sum_{kjk'j'} c_{kj} c_{k'j'}^* \delta(k-k') |k\rangle_A \langle k| \otimes |j\rangle_B \langle j'| \\ &= \sum_{kjj'} c_{kj} c_{k'j'}^* |k\rangle_A \langle k| \otimes |j\rangle_B \langle j'|. \end{aligned} \quad (\text{A32})$$

Then, by re-distributing the sum, we get

$$\begin{aligned} \rho_{A'B} &= \sum_k \left(\sum_j c_{kj} |kj\rangle \right) \otimes \left(\sum_{j'} c_{kj'}^* \langle kj'| \right) \\ &= \sum_k d_k \left(\sum_j \frac{c_{kj}}{\sqrt{d_k}} |kj\rangle \right) \otimes \left(\sum_{j'} \frac{c_{kj'}^*}{\sqrt{d_k}} \langle kj'| \right), \end{aligned} \quad (\text{A33})$$

where we have introduced $d_k := \sum_j |c_{kj}|^2$ in the last step (clearly $\sum_k d_k = 1$). Now introducing the pure state

$$|\eta_k\rangle := \sum_j \frac{c_{kj}}{\sqrt{d_k}} |kj\rangle, \quad (\text{A34})$$

we can write the following spectral decomposition for the output state

$$\rho_{A'B} = \sum_k d_k |\eta_k\rangle \langle \eta_k|. \quad (\text{A35})$$

In particular, note that we can always write the tensor product

$$|\eta_k\rangle = |k\rangle \otimes |\xi(k)\rangle, \quad |\xi(k)\rangle := \sum_j \frac{c_{kj}}{\sqrt{d_k}} |j\rangle, \quad (\text{A36})$$

so that the output state is manifestly in separable form

$$\rho_{A'B} = \sum_k d_k |k\rangle_{A'} \langle k| \otimes |\xi(k)\rangle_B \langle \xi(k)|. \quad (\text{A37})$$

Proof can trivially be extended to mixed states via their spectral decomposition into pure states.

5. $R_\theta \otimes R_\theta$ -invariant Gaussian states are separable

To derive the CM of Eq. (32) just check that a 2×2 real matrix \mathbf{M} is invariant under rotations $\mathbf{R}_\theta \mathbf{M} \mathbf{R}_\theta^T = \mathbf{M}$ (or, equivalently, it commutes with rotations $[\mathbf{M}, \mathbf{R}_\theta] = 0$) if and only if it takes the asymmetric form

$$\mathbf{M} = \begin{pmatrix} m & t \\ -t & m \end{pmatrix}, \quad (\text{A38})$$

with m, t real numbers. Thus, the $\mathbf{A}, \mathbf{B}, \mathbf{C}$ blocks of the CM (32) must have this general form, with the blocks \mathbf{A} and \mathbf{B} diagonal by imposing the additional condition of symmetry.

Then, it is easy to check that CM of Eq. (32) describes a separable Gaussian state. In fact, using suitable local rotations $\mathbf{R}_x \oplus \mathbf{R}_y$ (therefore not changing the separability properties of the state), we can transform \mathbf{V}_{AB} into the simpler form

$$\mathbf{V}'_{AB}(\alpha, \beta, \gamma) = \begin{pmatrix} \alpha \mathbf{I} & \gamma \mathbf{I} \\ \gamma \mathbf{I} & \beta \mathbf{I} \end{pmatrix}, \quad (\text{A39})$$

where $\gamma = \sqrt{\omega^2 + \varphi^2}$. Without loss of generality, suppose that $\beta \geq \alpha$ and set $\beta - \alpha := \delta$.

We can always generate ρ'_{AB} with CM $\mathbf{V}'_{AB}(\alpha, \beta, \gamma)$ by applying local Gaussian channels $\mathcal{I}_A \otimes \mathcal{G}_B$ to the symmetric Gaussian state ρ''_{AB} with CM $\mathbf{V}''_{AB} = \mathbf{V}'_{AB}(\alpha, \alpha, \gamma)$. It is sufficient to choose the identity channel \mathcal{I}_A and a Gaussian channel \mathcal{G}_B with additive noise δ (also known as canonical B2 form [14]). It is now trivial to check that the state ρ''_{AB} is separable. In fact, \mathbf{V}''_{AB} is a bona-fide quantum CM when its parameters α and γ satisfy the conditions $\alpha \geq 1$ and $|\gamma| \leq \alpha - 1$. Then, we can check that the partially-transposed symplectic eigenvalues of \mathbf{V}''_{AB} are greater than 1, i.e., the state is separable, when $|\gamma| \leq \sqrt{\alpha^2 - 1}$, which is a condition always satisfied. Finally, since ρ''_{AB} is separable, then also ρ'_{AB} and ρ_{AB} must be separable (local operations cannot create entanglement).

6. No entangled Gaussian state is invariant under $U \otimes U$ Gaussian twirlings

The proof is easy. Suppose that we have an arbitrary Gaussian state ρ_{AB} , with mean value $\bar{\mathbf{x}}_{AB}$ and covariance CM \mathbf{V}_{AB} . The action of two Gaussian unitaries $U \otimes U$ on ρ_{AB} corresponds to apply two identical displacements to its mean value

$$\bar{\mathbf{x}}_{AB} \rightarrow \bar{\mathbf{x}}_{AB} + (\mathbf{d}, \mathbf{d})^T, \quad (\text{A40})$$

and two identical symplectic matrices to its CM

$$\mathbf{V}_{AB} \rightarrow (\mathbf{S} \oplus \mathbf{S}) \mathbf{V}_{AB} (\mathbf{S} \oplus \mathbf{S})^T. \quad (\text{A41})$$

In general, there is no chance to find an invariant Gaussian state, since any nonzero displacement \mathbf{d} maps the input state into a different output state.

We then restrict the search to considering canonical Gaussian unitaries ($\mathbf{d} = \mathbf{0}$) which are one-to-one with the symplectic transformations. According to Euler's decomposition [14], any single-mode symplectic transformation \mathbf{S} can be decomposed into an orthogonal rotation \mathbf{R}_θ , a single-mode squeezing \mathbf{S}_r , and another orthogonal rotation \mathbf{R}_ω , where θ, ω are angles and $r \geq 1$ is a squeezing parameter. As long as some squeezing is present ($r > 1$), the trace of the CM changes (physically this corresponds to increase the mean number of photons). As a result, the CM and, therefore, the Gaussian state must change.

Thus, we are left to find Gaussian states which are invariant under rotations only (which are passive transformations, i.e., preserving the trace of the CM). However, we have already seen that, despite they exist, these Gaussian states must be separable.

Appendix B: Basic notions on bosonic systems and Gaussian states

In this appendix, we provide notions on bosonic systems, Gaussian states and their properties, which are

useful for understanding the mathematical details of the main part of the paper. In detail, we discuss Gaussian states and their statistical moments (Sec. B1), the symplectic manipulation of covariance matrices (Sec. B2), the bona-fide conditions for bipartite Gaussian states and their separability properties (Sec. B3), EPR correlations (Sec. B4) and, finally, the notions of discord and Gaussian discord (Sec. B5).

1. Gaussian states and operations: Representation in terms of the statistical moments

The most important systems in continuous variable quantum information are the bosonic modes of the electromagnetic field. A bosonic mode is a quantum system with an infinite-dimensional Hilbert space and described by a pair of quadrature operators: Position \hat{q} and momentum \hat{p} , satisfying the commutation relation $[\hat{q}, \hat{p}] = 2i$ (here we set $\hbar = 2$). More generally, a bosonic system of n modes is described by a vector of $2n$ quadrature operators

$$\hat{\mathbf{x}}^T := (\hat{q}_1, \hat{p}_1, \dots, \hat{q}_n, \hat{p}_n), \quad (\text{B1})$$

satisfying $[\hat{x}_i, \hat{x}_j] = 2i\Omega_{ij}$, where $i, j = 1, \dots, 2n$ and Ω_{ij} is the generic element of the symplectic form

$$\Omega := \bigoplus_{k=1}^n \begin{pmatrix} 0 & 1 \\ -1 & 0 \end{pmatrix}. \quad (\text{B2})$$

In experimental quantum optics, bosonic modes are typically prepared in Gaussian states. By definition, a quantum state ρ is ‘‘Gaussian’’ when its Wigner phase-space representation is Gaussian [14]. A Gaussian state is very easy to describe, being completely characterized by its first and second-order statistical moments.

The first-order moment is known as the mean value, and defined by $\bar{\mathbf{x}} := \langle \hat{\mathbf{x}} \rangle$, where $\langle \hat{O} \rangle := \text{Tr}(\hat{O}\rho)$ denotes the average of the arbitrary operator \hat{O} on the state ρ . The second-order moment is known as the covariance matrix (CM) \mathbf{V} , with generic element

$$V_{ij} := \frac{1}{2} \langle \{\Delta\hat{x}_i, \Delta\hat{x}_j\} \rangle, \quad (\text{B3})$$

where $\Delta\hat{x}_i := \hat{x}_i - \bar{x}_i$ is the deviation and $\{, \}$ is the anticommutator. Note that the diagonal elements V_{ii} are just the variances of the quadratures

$$V(\hat{x}_i) := \langle \Delta\hat{x}_i^2 \rangle = \langle \hat{x}_i^2 \rangle - \bar{x}_i^2. \quad (\text{B4})$$

The CM is a $2n \times 2n$ real symmetric matrix, which must satisfy the uncertainty principle [54]

$$\mathbf{V} + i\Omega \geq 0, \quad (\text{B5})$$

implying the positive-definiteness $\mathbf{V} > 0$ [45].

The simplest Gaussian states are thermal states. A single-mode thermal state has zero mean and CM $\mathbf{V} =$

$(2\bar{n} + 1)\mathbf{I}$, where \mathbf{I} is the 2×2 identity matrix and $\bar{n} \geq 0$ is the mean number of thermal photons (vacuum state for $\bar{n} = 0$). Multimode thermal states are constructed by tensor product. Tensor product of states $\rho_1 \otimes \rho_2$ corresponds to direct sum of CMs $\mathbf{V}_1 \oplus \mathbf{V}_2$. Conversely, the partial trace $\rho_1 = \text{Tr}_2(\rho_{12})$ corresponds to collapsing the total CM \mathbf{V}_{12} into the block \mathbf{V}_1 spanned by (\hat{q}_1, \hat{p}_1) .

In the experimental practice, Gaussian states are typically processed by Gaussian operations. The simplest ones are Gaussian unitaries, defined as those unitary operators which transform Gaussian states into Gaussian states. At the level of the statistical moments, the action of a Gaussian unitary $\rho \rightarrow U\rho U^\dagger$ corresponds to

$$\bar{\mathbf{x}} \rightarrow \mathbf{S}\bar{\mathbf{x}} + \mathbf{d}, \quad \mathbf{V} \rightarrow \mathbf{S}\mathbf{V}\mathbf{S}^T, \quad (\text{B6})$$

where \mathbf{d} is a real displacement vector and \mathbf{S} is a symplectic matrix, i.e., a real matrix preserving the symplectic form $\mathbf{S}\Omega\mathbf{S}^T = \Omega$. In the Heisenberg picture, a Gaussian unitary corresponds to the affine map

$$\hat{\mathbf{x}} \rightarrow \mathbf{S}\hat{\mathbf{x}} + \mathbf{d}. \quad (\text{B7})$$

In particular, a Gaussian unitary is called ‘‘canonical’’ when $\mathbf{d} = \mathbf{0}$. The most important example of canonical unitary is the beam-splitter transformation, which involves two bosonic modes. This unitary is characterized by the symplectic matrix

$$\mathbf{S}(\tau) = \begin{pmatrix} \sqrt{\tau}\mathbf{I} & \sqrt{1-\tau}\mathbf{I} \\ -\sqrt{1-\tau}\mathbf{I} & \sqrt{\tau}\mathbf{I} \end{pmatrix}, \quad (\text{B8})$$

with transmissivity parameter $0 \leq \tau \leq 1$.

Other important examples of Gaussian operations are the Gaussian channels [46]. These channels describe all those cases where bosonic systems and environment interact by means of linear and/or bilinear Hamiltonians. The action of a Gaussian channel $\rho \rightarrow \mathcal{E}(\rho)$ corresponds to the following transformation for the CM of the state

$$\mathbf{V} \rightarrow \mathbf{K}\mathbf{V}\mathbf{K}^T + \mathbf{N}, \quad (\text{B9})$$

where \mathbf{K} and $\mathbf{N} = \mathbf{N}^T$ are $2n \times 2n$ real matrices, satisfying the condition $\mathbf{N} + i\Omega - i\mathbf{K}\Omega\mathbf{K}^T \geq 0$ [47].

The most important example of Gaussian channel is the lossy channel, which is typically used to model the optical propagation through dissipative linear media. When a single bosonic mode propagates through a lossy channel, its CM is transformed by Eq. (B9) with

$$\mathbf{K} = \sqrt{\tau}\mathbf{I}, \quad \mathbf{N} = (1 - \tau)(2\bar{n} + 1)\mathbf{I}, \quad (\text{B10})$$

where $0 \leq \tau \leq 1$ is the transmissivity of the channel and $\bar{n} \geq 0$ its thermal number. A single-mode lossy channel can always be dilated into a beam-splitter with transmissivity τ , which mixes the incoming mode with an environmental thermal mode with \bar{n} mean photons.

2. Symplectic spectrum

A central result in the theory of Gaussian states is Williamson's theorem [14, 48]. Given a CM \mathbf{V} , there is a symplectic matrix \mathbf{S} realizing the diagonalization

$$\mathbf{V} = \mathbf{S}\mathbf{W}\mathbf{S}^T, \quad \mathbf{W} = \bigoplus_{k=1}^n \nu_k \mathbf{I}, \quad (\text{B11})$$

where the diagonal matrix \mathbf{W} is known as the Williamson normal form, and $\{\nu_1, \dots, \nu_n\}$ are the n symplectic eigenvalues of the CM. Since $\det \mathbf{S} = 1$, we have that

$$\det \mathbf{V} = \prod_{k=1}^n \nu_k^2. \quad (\text{B12})$$

Using the symplectic spectrum, we can write the uncertainty principle of Eq. (B5) in the equivalent form

$$\mathbf{V} > 0, \quad \nu_k^2 \geq 1, \quad (\text{B13})$$

which implies $\nu_k \geq 1$ [49]. The symplectic spectrum fully determines the entropic and purity properties of the Gaussian states. In fact, the von Neumann entropy $S(\rho) := -\text{Tr}(\rho \log \rho)$ of an arbitrary n -mode Gaussian state is expressed by [14]

$$S(\rho) = \sum_{k=1}^n h(\nu_k), \quad (\text{B14})$$

where the function $h(x)$ is given in Eq. (49), with the logarithmic base equal to 2 for bits or “ e ” for nats. The purity of a Gaussian state is given by

$$\mu_p(\rho) := \text{Tr} \rho^2 = \frac{1}{\sqrt{\det \mathbf{V}}} = \prod_{k=1}^n \nu_k^{-1}, \quad (\text{B15})$$

so that the state is pure (mixed) iff $\det \mathbf{V} = 1$ (> 1).

In our paper, we consider situations where the symplectic eigenvalues are large. In this case, it is useful to use the asymptotic expansion

$$h(x) \simeq \log \frac{e}{2} x + O\left(\frac{1}{x}\right), \quad (\text{B16})$$

which is valid for large x . In particular, if the whole symplectic spectrum is diverging (ν_k large for any k), then we can use Eq. (B16) to write the asymptotic formula

$$S(\rho) \simeq \log \left(\frac{e}{2}\right)^n \sqrt{\det \mathbf{V}} = \log \frac{1}{\mu_p(\rho)} + n \log \frac{e}{2}, \quad (\text{B17})$$

where the entropy is directly related to the purity of the Gaussian state.

3. Two-mode Gaussian states and bipartite entanglement

Since we are interested in the distribution of bipartite entanglement, we devote a specific section to Gaussian states of two bosonic modes and their separability properties. Let us consider two modes, A and B , with quadrature vector $\hat{\mathbf{x}}^T := (\hat{q}_A, \hat{p}_A, \hat{q}_B, \hat{p}_B)$. We assume that these modes are described by a zero-mean Gaussian state ρ_{AB} . Since $\bar{\mathbf{x}} = \mathbf{0}$, this state is fully characterized by its CM, that we can always express in the blockform

$$\mathbf{V} = \begin{pmatrix} \mathbf{A} & \mathbf{C} \\ \mathbf{C}^T & \mathbf{B} \end{pmatrix}, \quad (\text{B18})$$

where \mathbf{A} , \mathbf{B} and \mathbf{C} are 2×2 matrices. Finding the symplectic spectrum is straightforward, since [14, 51]

$$\nu_{\pm} = \sqrt{\frac{\Delta \pm \sqrt{\Delta^2 - 4 \det \mathbf{V}}}{2}}, \quad (\text{B19})$$

where $\Delta := \det \mathbf{A} + \det \mathbf{B} + 2 \det \mathbf{C}$. The uncertainty principle is then equivalent to the bona-fide condition

$$\mathbf{V} > 0, \quad \nu_{-}^2 \geq 1, \quad (\text{B20})$$

where ν_{-} is the smallest symplectic eigenvalue.

As an example, consider the two-mode CM of the form

$$\mathbf{V} = \begin{pmatrix} \omega & & g & \\ & \omega & & g' \\ g & & \omega & \\ & g' & & \omega \end{pmatrix} \quad (\text{B21})$$

where $\omega \geq 1$ quantifies the thermal noise present in each mode, while g and g' are cross-correlation parameters. This is the CM of the correlated-noise Gaussian environment which is defined in the main text [see Eq. (38)]. It is easy to derive simple bona-fide conditions in terms of the parameters ω , g and g' . In particular, given $\omega \geq 1$, we can easily derive conditions for the two correlation parameters, by imposing Eq. (B20). The positivity $\mathbf{V} > 0$ is equivalent to the positivity of the principal minors of the matrix. The positivity of the first two minors is trivially implied by $\omega \geq 1$. The third minor gives

$$\det \begin{pmatrix} \omega & 0 & g \\ 0 & \omega & 0 \\ g & 0 & \omega \end{pmatrix} > 0 \Leftrightarrow \omega(\omega^2 - g^2) > 0, \quad (\text{B22})$$

which is equivalent to

$$|g| < \omega. \quad (\text{B23})$$

The fourth minor corresponds to the determinant

$$\det \mathbf{V} = (\omega^2 - g^2)(\omega^2 - g'^2), \quad (\text{B24})$$

and its positivity $\det \mathbf{V} > 0$ leads to the condition

$$|g'| < \omega. \quad (\text{B25})$$

We then derive the symplectic spectrum of the CM (B21), which is given by

$$\nu_{\pm} = \sqrt{\omega^2 + gg' \pm \omega |g + g'|} . \quad (\text{B26})$$

Now, we find that $\nu_{-}^2 \geq 1$ is equivalent to [52]

$$\omega^2 + gg' - 1 \geq \omega |g + g'| . \quad (\text{B27})$$

Thus, an environmental CM of the form (B21) with thermal noise $\omega \geq 1$ is a bona-fide CM if the correlation parameters g and g' satisfy the three bona-fide conditions of Eqs. (B23), (B25) and (B27) which are also given in Eq. (40) of the main text. Using Eqs. (B15) and (B24), we also see that the purity of the Gaussian state with CM (B21) is given by

$$\mu_p = [(\omega^2 - g^2)(\omega^2 - g'^2)]^{-1/2} . \quad (\text{B28})$$

Its von Neumann entropy is computed by using Eq. (B14) and the spectrum in Eq. (B26).

It is easy to study the separability properties of an arbitrary two-mode Gaussian state with CM in the generic blockform of Eq. (B18). In fact, it is sufficient to compute the smallest partially-transposed symplectic (PTS) eigenvalue ε . This eigenvalue can be computed using the formula of ν_{-} , given in Eq. (B19), proviso that we replace Δ with $\tilde{\Delta} = \det \mathbf{A} + \det \mathbf{B} - 2 \det \mathbf{C}$. Then, a Gaussian state is separable (entangled) if and only if $\varepsilon \geq 1$ ($\varepsilon < 1$). More strongly, this eigenvalue provides a quantification of entanglement, being an entanglement monotone for two-mode Gaussian states. In fact, it is monotonically related to the log-negativity $\mathcal{N} = \max\{0, -\log \varepsilon\}$, which is another entanglement monotone and can be expressed in entanglement bits (ebits).

The log-negativity \mathcal{N} provides an upper-bound to the distillable entanglement, corresponding to the average number of ebits per copy which can be extracted from infinitely-many copies of the state $\rho_{AB} \otimes \rho_{AB} \otimes \dots$. We can also consider a lower-bound to distillable entanglement. According to the hashing inequality [55, 56], this lower bound is given by the coherent information [57, 58]

$$I(A)B = S(\rho_B) - S(\rho_{AB}) , \quad (\text{B29})$$

where $\rho_B = \text{Tr}_A(\rho_{AB})$ is the reduced state of Bob, here corresponding to a zero-mean Gaussian state with CM \mathbf{B} . Using Eq. (B14), the coherent information becomes

$$I(A)B = h(\nu_B) - h(\nu_{-}) - h(\nu_{+}) , \quad (\text{B30})$$

where $\nu_B = \sqrt{\det \mathbf{B}}$ is the symplectic eigenvalue of \mathbf{B} , and $\{\nu_{-}, \nu_{+}\}$ is the symplectic spectrum of \mathbf{V} . In the case where these eigenvalues are all large, we can use the expansion of Eq. (B16) to get the formula

$$I(A)B \simeq \log \frac{2}{e} \sqrt{\frac{\det \mathbf{B}}{\det \mathbf{V}}} . \quad (\text{B31})$$

More precisely, the coherent information is a lower bound to the distillable entanglement which is achievable

by means of one-way protocols between Alice and Bob (one-way distillability). In these protocols, Alice applies a quantum instrument to her copies, i.e., a collection of completely-positive trace-preserving maps labelled by a classical index k . Then, she classically communicates k to Bob, who applies a conditional quantum operation on his copies (see Ref. [55] for more details).

4. EPR correlations

The most important example of two-mode Gaussian state is the two-mode squeezed vacuum state, also known as the EPR state. This state represents the most common source of continuous-variable entanglement.

An EPR state has zero mean and CM given by Eq. (33) in the main text. The quadratures $\hat{\mathbf{x}}^T := (\hat{q}_A, \hat{p}_A, \hat{q}_B, \hat{p}_B)$ have equal variances

$$\langle \hat{q}_A^2 \rangle = \dots = \langle \hat{p}_B^2 \rangle = \mu \geq 1 , \quad (\text{B32})$$

and maximal correlations

$$\langle \hat{q}_A \hat{q}_B \rangle = -\langle \hat{p}_A \hat{p}_B \rangle = \mu' := \sqrt{\mu^2 - 1} . \quad (\text{B33})$$

The parameter μ can be used to quantify the entanglement between the two modes A and B . In fact, the smallest PTS eigenvalue takes the form

$$\varepsilon = \sqrt{2\mu(\mu - \mu') - 1} , \quad (\text{B34})$$

which is monotonically decreasing in μ . We can easily check that we have entanglement ($\varepsilon < 1$) for any $\mu > 1$.

The EPR correlations can be characterized in terms of the variance of the EPR quadratures

$$\hat{q}_{-} := \frac{\hat{q}_A - \hat{q}_B}{\sqrt{2}} , \quad \hat{p}_{+} := \frac{\hat{p}_A + \hat{p}_B}{\sqrt{2}} . \quad (\text{B35})$$

The EPR condition corresponds to $V(\hat{q}_{-}) = V(\hat{p}_{+}) < 1$, which means that the quadrature correlations between the two modes are below the vacuum noise. For the EPR state described by Eq. (33) indeed we have

$$V(\hat{q}_{-}) = V(\hat{p}_{+}) = \mu - \mu' , \quad (\text{B36})$$

which is less than 1 for any $\mu > 1$. For this type of state, EPR correlations and entanglement are equivalent conditions. In general, for an arbitrary two-mode Gaussian state, the presence of EPR correlations is only a sufficient condition for entanglement.

In the limit of large entanglement ($\mu \rightarrow \infty$), the EPR state becomes ideal. In fact, we have $V(\hat{q}_{-}) = V(\hat{p}_{+}) \rightarrow 0$, which corresponds to realizing the ideal EPR correlations $\hat{q}_A = \hat{q}_B$ and $\hat{p}_A = -\hat{p}_B$, where positions (momenta) are perfectly correlated (anticorrelated). Note that an alternative EPR state can be defined using the other reflection matrix $-\mathbf{Z}$ in the place of \mathbf{Z} in Eq. (33). This alternative state has EPR correlations in the quadratures \hat{q}_{+} and \hat{p}_{-} , therefore tending to realize the ideal conditions $\hat{q}_A = -\hat{q}_B$ and $\hat{p}_A = \hat{p}_B$. In our work, we do not consider this state, but similar results can easily be derived.

5. Quantum discord and Gaussian discord

Quantum entanglement is synonymous of quantum correlations for pure states. For mixed states the scenario is more subtle. In fact, separable mixed states may still contain features of quantumness, one of which is known as quantum discord [34, 59, 60]. Quantum discord derives from different quantum extensions of the notion of classical mutual information.

Classically, the mutual information of two random classical variables, A and B , is defined as

$$I(A : B) = H(A) + H(B) - H(A, B) , \quad (\text{B37})$$

where H is the Shannon entropy. Using the chain rule for the entropy, we can also write the equivalent formulation

$$I(A : B) = H(A) - H(A|B) , \quad (\text{B38})$$

where $H(\dots)$ is the conditional Shannon entropy.

In quantum mechanics, we can have two inequivalent generalizations, the first being provided by the quantum mutual information which accounts for the total correlations present in a bipartite state ρ_{AB} . It is expressed in terms of the von Neumann entropy as

$$I(\rho_{AB}) = S(\rho_A) + S(\rho_B) - S(\rho_{AB}) . \quad (\text{B39})$$

Another generalization is given by the entropic quantity

$$C(\rho_{AB}) = S(\rho_A) - \inf_{\mathcal{M}_B} S(A|\mathcal{M}_B) , \quad (\text{B40})$$

where $\mathcal{M}_B = \{M_k\}$ is a POVM acting on system B and

$$S(A|\mathcal{M}_B) := \sum_k p_k S(\rho_{A|k}) , \quad (\text{B41})$$

where p_k is the probability of the outcome k and $\rho_{A|k} := \text{Tr}_B(\rho_{AB}M_k)$ is the conditional state of A .

The quantity $C(\rho_{AB})$, which is expressed in bits or classical bits (cbits), quantifies the classical correlations within the state, corresponding to the maximal amount of

common randomness which can be extracted using local operations and one-way classical communication [61].

Quantum discord aims to quantify the quantum correlations in the state. Thus, it is defined as the difference between total and classical correlations

$$D(\rho_{AB}) = I(\rho_{AB}) - C(\rho_{AB}) , \quad (\text{B42})$$

and measured in bits or discordant bits (dbits). It is important to note that Eq. (B40) is generally non-symmetric under system permutation. As a result, we have that the B -type quantities $C(\rho_{BA})$ and $D(\rho_{BA})$ are generally different from the A -type quantities of Eqs. (B40) and (B42). Such ambiguity clearly disappears for symmetric states ($\rho_{AB} = \rho_{BA}$), as the states considered in our paper.

For bosonic states, one can define the Gaussian discord by restricting the previous minimization from arbitrary to Gaussian POVMs [62, 63]. It is clear that Gaussian discord represents an upper bound to the actual discord, and the classical correlations of Eq. (B40) restricted to Gaussian POVMs represent a lower bound to the actual classical correlations of the state. Gaussian discord is conjectured to be the actual discord in the case of bosonic Gaussian states, for which we know closed formulas [62, 63]. In fact, consider a two-mode Gaussian state with CM in the blockform of Eq. (B18) and symplectic spectrum $\{\nu_-, \nu_+\}$. Then, the (restricted) classical correlations and Gaussian discord are given by

$$C(\rho_{AB}) = h\left(\sqrt{\det \mathbf{A}}\right) - \Sigma , \quad (\text{B43})$$

$$D(\rho_{AB}) = h\left(\sqrt{\det \mathbf{B}}\right) - h(\nu_-) - h(\nu_+) + \Sigma , \quad (\text{B44})$$

where the expression of the Σ -term is given in Ref. [63]. Apart from the specific case of tensor-product states $\rho_{AB} = \rho_A \otimes \rho_B$, all two-mode Gaussian states have non-zero Gaussian discord [63] and non-zero (actual) discord [64]. In particular, Gaussian discord $D > 1$ implies the presence of entanglement [63].

-
- [1] M. A. Nielsen and I. L. Chuang, *Quantum Computation and Quantum Information* (Cambridge University Press, Cambridge, 2000).
- [2] M. M. Wilde, *Quantum Information Theory* (Cambridge University Press, Cambridge 2013). Preprint arXiv:1106.1445.
- [3] C. Bennett, G. Brassard, C. Crepeau, R. Jozsa, A. Peres, and W. K. Wootters, Phys. Rev. Lett. **70**, 1895 (1993).
- [4] A. Furusawa, J. L. Sørensen, S. L. Braunstein, C. A. Fuchs, H. J. Kimble, and E. S. Polzik, Science **282**, 706 (1998).
- [5] M. A. Nielsen and I. L. Chuang, Phys. Rev. Lett. **79**, 321 (1997).
- [6] A. K. Ekert, Phys. Rev. Lett. **67**, 661 (1991).
- [7] N. Gisin, G. Ribordy, W. Tittel, and H. Zbinden, Rev. Mod. Phys. **74**, 145 (2002).
- [8] C. H. Bennett, J. H. Bernstein, S. Popescu, and B. Schumacher, Phys. Rev. A **53**, 2046-2052 (1996).
- [9] C. H. Bennett, G. Brassard, S. Popescu, B. Schumacher, J. A. Smolin, and W. K. Wootters, Phys. Rev. A **76**, 722-725 (1996).
- [10] M. Horodecki, P. W. Shor, and M. B. Ruskai, Rev. Math. Phys. **15**, 629-641 (2003).
- [11] A. S. Holevo, Problems of Information Transmission **44**, 3-18 (2008).
- [12] S. L. Braunstein and A. K. Pati, *Quantum Information Theory with Continuous Variables* (Kluwer Academic, Dordrecht, 2003).

- [13] S. L. Braunstein and P. van Loock, *Rev. Mod. Phys.* **77**, 513 (2005).
- [14] C. Weedbrook, S. Pirandola, R. Garcia-Patron, N. J. Cerf, T. C. Ralph, J. H. Shapiro, and S. Lloyd, *Rev. Mod. Phys.* **84**, 621 (2012).
- [15] In general, a decoherence-free subspace is a subspace of the state-space which evolves unitarily under the action of the quantum channel. This subspace is invariant when no evolution occurs.
- [16] H.-P. Breuer and F. Petruccione, *The Theory of Open Quantum Systems* (Oxford University Press, Oxford, 2002).
- [17] U. Weiss, *Quantum Dissipative Systems* (World Scientific, Singapore, 2008).
- [18] R. Werner, *Phys. Rev. A* **40**, 4277 (1989).
- [19] M. Horodecki and P. Horodecki, *Phys. Rev. A* **59**, 4206–4216 (1999).
- [20] A. Einstein, B. Podolsky, and N. Rosen, *Phys. Rev.* **47**, 777 (1935).
- [21] L. Mišta, Jr., R. Filip, and J. Fiurásek, *Phys. Rev. A* **65**, 062315 (2002).
- [22] F. Caruso, V. Giovannetti, C. Lupo, and S. Mancini, preprint arXiv:1207.5435.
- [23] S. Bose, *Phys. Rev. Lett.* **91**, 207901 (2003).
- [24] G. Benenti, A. D’Arrigo, and G. Falci, *Phys. Rev. Lett.* **103**, 020502 (2009).
- [25] K. H. Madsen, S. Ates, T. Lund-Hansen, A. Löffler, S. Reitzenstein, A. Forchel, and P. Lodahl, *Phys. Rev. Lett.* **106**, 233601 (2011).
- [26] J. H. Shapiro, *IEEE J. Sel. Top. Quantum Electron.* **15**, 1547 (2009).
- [27] C. Lupo, V. Giovannetti, S. Pirandola, S. Mancini, and S. Lloyd, *Phys. Rev. A* **84**, 010303(R) (2011).
- [28] C. Lupo, V. Giovannetti, S. Pirandola, S. Mancini, and S. Lloyd, *Phys. Rev. A* **85**, 062314 (2012).
- [29] C. Lupo, S. Pirandola, V. Giovannetti, and S. Mancini, *Phys. Rev. A* **87**, 062310 (2013).
- [30] G. A. Tyler, and R. W. Boyd, *Opt. Lett.* **34**, 142 (2009).
- [31] A. A. Semenov and W. Vogel, *Phys. Rev. A* **80**, 021802 (2009).
- [32] R. W. Boyd, B. Rodenburg, M. Mirhosseini, and S. M. Barnett, *Opt. Express* **19**, 18310 (2011).
- [33] In fact, the global input state $\rho_{AB} \otimes \rho_{E_2}$ has CM $\mathbf{V}_{AB}(\mu) \oplus \omega \mathbf{I}$. This CM is subject to the symplectic transformation $\mathbf{I} \oplus \mathbf{S}(\tau)$, where $\mathbf{S}(\tau)$ is the beam splitter matrix of Eq. (B8) acting on modes B and E_2 . Tracing out the environment from the output CM, we get Eq. (62).
- [34] K. Modi, A. Brodutch, H. Cable, T. Paterek, and V. Vedral, *Rev. Mod. Phys.* **84**, 1655–1707 (2012).
- [35] M. Sacchi, *Phys. Rev. A* **72**, 014305 (2005).
- [36] Ch. Spengler, M. Huber and B.C. Hiesmayr, *J. Phys. A: Math. Theor.* **43**, 385306 (2010).
- [37] C. Dankert, *Efficient Simulation of Random Quantum States and Operators*, MSc thesis, University of Waterloo (2005). See also arXiv quant-ph/0512217.
- [38] C. Dankert, R. Cleve, J. Emerson and E. Livine, *Phys. Rev. A* **80**, 012304 (2009).
- [39] D. Gross, K. Audenaert, J. Eisert, *J. Math. Phys.* **48**, 052104 (2007).
- [40] D. P. DiVincenzo, D. W. Leung, and B. M. Terhal, *IEEE Trans. on Inf. Theory* **48**, 580–599 (2002).
- [41] D. Gottesman, *Stabilizer Codes and Quantum Error Correction*, Ph.D. thesis, CalTech (1997).
- [42] A. R. Calderbank, E. M. Rains, P. W. Shor, and N. J. A. Sloane, *IEEE Trans. on Inf. Theory* **44**, 1369–1387 (1998).
- [43] G. Chiribella, *Optimal Estimation of Quantum Signals in the Presence of Symmetry*, PhD thesis, Pavia (2006).
- [44] B. Synak, K. Horodecki, and M. Horodecki, *J. Math. Phys.* **46**, 082107 (2005).
- [45] S. Pirandola, A. Serafini, and S. Lloyd, *Phys. Rev. A* **79**, 052327 (2009).
- [46] A. S. Holevo, M. Sohma, and O. Hirota, *Phys. Rev. A* **59**, 1820 (1999).
- [47] A. S. Holevo and R. F. Werner, *Phys. Rev. A* **63**, 032312 (2001).
- [48] J. Williamson, *Am. J. Math.* **58**, 141 (1936).
- [49] Note that the uncertainty principle is known to be equivalent to the bona-fide condition $\mathbf{V} > 0$ and $\nu_k \geq 1$ [14]. However, since $\mathbf{V} > 0$ and \mathbf{W} is congruent with \mathbf{V} , then it is automatically implied that \mathbf{W} has strictly-positive eigenvalues (this is a simple consequence of Sylvester’s law of inertia [50]). As a result, we have that $\nu_k \geq 1$ is equivalent to $\nu_k^2 \geq 1$ and, therefore, the previous bona-fide condition can also be stated as in Eq. (B13).
- [50] R. Bathia, *Positive Definite Matrices* (Princeton University Press, Princeton, 2007).
- [51] A. Serafini, F. Illuminati, and S. De Siena, *J. Phys. B* **37**, L21 (2004).
- [52] Note that Eq. (B27) does not imply Eqs. (B23) and (B25). For instance, if we set $g' = g = \omega + d$ with $d \geq 1$, then Eq. (B27) becomes $d^2 - 1 \geq 0$ which is always satisfied. In other words, Eq. (B27) alone is not sufficient to guarantee the bona-fide of the CM.
- [53] G. Vidal and R. F. Werner, *Phys. Rev. A* **65**, 032314 (2002).
- [54] R. Simon, N. Mukunda, and B. Dutta, *Phys. Rev. A* **49**, 1567 (1994).
- [55] I. Devetak and A. Winter, *Phys. Rev. Lett.* **93**, 080501 (2004).
- [56] I. Devetak and A. Winter, *Proc. R. Soc. Lond. A* **461**, 207 (2005).
- [57] B. Schumacher and M. A. Nielsen, *Phys. Rev. A* **54**, 2629 (1996).
- [58] S. Lloyd, *Phys. Rev. A* **55**, 1613 (1997).
- [59] H. Ollivier and W. H. Zurek, *Phys. Rev. Lett.* **88**, 017901 (2001).
- [60] L. Henderson and V. Vedral, *J. Phys. A* **34**, 6899 (2001).
- [61] I. Devetak and A. Winter, *IEEE Trans. Inform. Theory* **50**, 3183, (2004).
- [62] P. Giorda and M. G. A. Paris, *Phys. Rev. Lett.* **105**, 020503 (2010).
- [63] G. Adesso and A. Datta, *Phys. Rev. Lett.* **105**, 030501 (2010).
- [64] S. Rahimi-Keshari, C. M. Caves, and T. C. Ralph, *Phys. Rev. A* **87**, 012119 (2013).
- [65] P. Giorda, M. Allegra, and M. G. A. Paris, *Phys. Rev. A* **86**, 052328 (2012).
- [66] S. Olivares and M. G. A. Paris, *Int. J. Mod. Phys. B* **27**, 1245024 (2012).
- [67] A. Peres, *Phys. Rev. Lett.* **77**, 1413–1415 (1996).
- [68] M. Horodecki, P. Horodecki, R. Horodecki, *Physics Letters A* **223**, 1–8 (1996).
- [69] Minor remark on matrix notation. We use ρ_{ijkl} when we refer to kets $|i, j\rangle$ and bras $\langle k, l|$. We prefer to use ρ_{ij}^{kl} when we distinguish between system A ($|i\rangle_A \langle j|$) and system B ($|k\rangle_B \langle l|$). Clearly, we have $\rho_{ijkl} = \rho_{ik}^{jl}$.

- [70] T. S. Cubitt, F. Verstraete, W. Dür, and J. I. Cirac, Phys. Rev. Lett. **91**, 037902 (2003).
- [71] A. Streltsov, H. Kampermann, and D. Bruß, Phys. Rev. Lett. **108**, 250501 (2012).
- [72] T. K. Chuan, J. Maillard, K. Modi, T. Paterek, M. Paternostro, and M. Piani, Phys. Rev. Lett. **109**, 070501 (2012).
- [73] L. Mišta, Jr. and N. Korolkova, Phys. Rev. A **77**, 050302 (2008).
- [74] L. Mišta, Jr., R. Filip, and J. Fiurášek, Phys. Rev. A **65**, 062315 (2002).
- [75] S. Pirandola, C. Ottaviani et al., in preparation.
- [76] C. H. Bennett, D. P. DiVincenzo, J. A. Smolin, and W. K. Wootters, Phys. Rev. A **54**, 3824 (1996).
- [77] G. Giedke, M.M.Wolf, O. Krüger, R. F.Werner, and J. I. Cirac, Phys. Rev. Lett. **91**, 107901 (2003).
- [78] G. Adesso, and F. Illuminati, Phys. Rev. A **72**, 032334 (2005).
- [79] C. Bény and O. Oreshkov, Phys. Rev. Lett. **104**, 120501 (2010).
- [80] In fact, for $d = 2$, we have $(I_{AB} + \mu V) = (\mu + 1)I_{AB} - 2\mu |-\rangle_{AB} \langle -|$ which, replaced in Eq. (20), gives the state of Eq. (9) by setting $\gamma = -\mu/(2 + \mu)$.
- [81] In all the paper, “log” is intended to be base 2, so that the corresponding quantities are measured in bits. We write “ln” for the natural base e .